Research Square

Preprints are preliminary reports that have not undergone peer review.
They should not be considered conclusive, used to inform clinical practice,
or referenced by the media as validated information.

Chemically Characterized Nanoencapsulated Homalomena aromatica Schott. Essential oil as Green Preservative Against Fungal and Aflatoxin B1 Contamination of Stored Spices based on in Vitro and in Situ Efficacy and Favourable Safety Profile on Mice

Shikha Tiwari
Banaras Hindu University Department of Botany
Neha Upadhyay
Banaras Hindu University Department of Botany
Bijendra Kumar Singh
Banaras Hindu University Department of Botany
Vipin Kumar Singh
Banaras Hindu University Department of Botany
Nawal Kishore Dubey (nkdubeybhu@gmail.com)
Banaras Hindu University https://orcid.org/0000-0002-7901-4696

Research Article

Keywords: Aflatoxin B1, Chitosan, Homalomena aromatica essential oil, Methylglyoxal, Nanoencapsulation

Posted Date: April 26th, 2021

DOI: https://doi.org/10.21203/rs.3.rs-421736/v1

License: This work is licensed under a Creative Commons Attribution 4.0 International License.
Read Full License

Version of Record: A version of this preprint was published at Environmental Science and Pollution Research on August 12th, 2021. See the published version at https://doi.org/10.1007/s11356-021-15794-2.

Title: Chemically characterized nanoencapsulated *Homalomena aromatica* Schott. essential oil as green preservative against fungal and aflatoxin B_1 contamination of stored spices based on *in vitro* and *in situ* efficacy and favourable safety profile on mice

Authors: Shikha Tiwari, Neha Upadhyay, Bijendra Kumar Singh, Vipin Kumar Singh and Nawal Kishore Dubey[1]*

Affiliation: Laboratory of Herbal Pesticides, Centre of Advanced study (CAS) in Botany, Institute of Science, Banaras Hindu University, Varanasi-221005, India

*Corresponding Author, Tel.: +919415295765. E-mail: nkdubeybhu@gmail.com (N.K. Dubey)

Abstract

Present study deals with the efficacy of nanoencapsulated *Homalomena aromatica* essential oil (HAEO) as a potent green preservative against toxigenic *Aspergillus flavus* strain (AF-LHP-NS 7), AFB_1 and free radical mediated deterioration of stored spices. GC-MS analysis revealed linalool (68.51%) as the major component of HAEO. HAEO was encapsulated into chitosan nanomatrix (CS-HAEO-Ne) and characterized through SEM, FTIR and XRD. CS-HAEO-Ne completely inhibited *A. flavus* growth and AFB_1 biosynthesis at 1.25 µL/mL and 1.0 µL/mL, respectively in comparison to unencapsulated HAEO (1.75 µL/mL and 1.25 µL/mL respectively). CS-HAEO-Ne exhibited superior antioxidant efficacy ($IC_{50\ (DPPH)}$ = 4.5 µL/mL) over unencapsulated HAEO ($IC_{50\ (DPPH)}$ = 15.9 µL/mL). Further, CS-HAEO-Ne caused significant reduction in ergosterol content in treated *A. flavus* and provoked leakage of cellular ions (Ca^{+2}, Mg^{+2} and K^{+}) as well as 260 nm and 280 nm absorbing materials. Depletion of methylglyoxal level in treated *A. flavus* cells deals with the novel antiaflatoxigenic efficacy of CS-HAEO-Ne. CS-HAEO-Ne depicted excellent *in situ* efficacy by inhibiting mold attack and AFB_1 contamination, mineral preservation and acceptable sensorial profile. Moreover, broad safety paradigm (LD_{50} value = 8006.84 µL/kg) of CS-HAEO-Ne also suggest it as novel green preservative to enhance shelf life of stored spices.

Keywords: Aflatoxin B_1, Chitosan, *Homalomena aromatica* essential oil, Methylglyoxal, Nanoencapsulation

Introduction

Spices are aromatic food commodities obtained from different plant parts such as root, seed, leaves, bark, flower, bulb, and fruit that are used all over world in food preparations (Thanushree et al. 2019). Peculiar flavor, colour and aromatic attributes of spices make them highly demanding food ingredient globally. In addition, several spices have been reported for their antimicrobial and antioxidant potential, along with vast therapeutic values such as analgesic, antipyretic, blood purifier, hepatoprotective, carminative, anticancerous, antidiabetic and anti-inflammatory (Gupta 2010; Singh et al. 2020a).

Unscientific and inappropriate harvesting, drying and storage techniques as well as warm and humid environmental conditions of storage make spices highly prone towards contamination by mold and their associated mycotoxins. Spices are reported to be second highly mycotoxin contaminated food item after nut products and fruits and vegetables (RASFF 2019). Among wide array of mycotoxins reported from different stored spices such as aflatoxins, citrinin, fumonisins, zearalenone, sterigmatocystin, tenuazonic, alternariol and deoxynivalenol (Pickova et al. 2020), aflatoxins are reported to be the most prevailing spice contaminant (Potorti et al. 2020). Aflatoxins, especially aflatoxin B_1 (AFB_1) contamination in stored spices has become a matter of great concern due to its potential properties of hepatocarcinogen, mutagen, teratogen, nephrotoxic and immunosuppressive agent for which it has been categorized as group 1 human carcinogen by International Agency for Research on Cancer (IARC 2012). Stringent regulations have been imposed by Food and Agricultural Organization (FAO) for the maximum acceptable limit of AFB_1 in spices and set as 5 µg/kg (FAO 2004). Yang et al. (2017) reported that fungal and mycotoxin contamination causes depletion of bioactive components of spices, thereby deteriorating spice quality. Moreover, AFB_1 contamination further provokes oxidative stress

resulting to rancidity and degradation of nutritive constituents of food items (Kovesi et al. 2020). Oxidative stress also enhances biosynthesis of methylglyoxal, the AFB_1 inducer molecule. Hence, in order to mitigate biodeterioration of food products caused due to fungal and mycotoxin contamination, chemicals such as butylated derivatives, potassium sorbate, and propyl gallate have been widely used. However, issues of environmental toxicity, resistance development, residual toxicity and carcinogenic effects (Rajkumar et al. 2020a) greatly limit their applicability. On the contrary, plant based green preservatives have been considered as better alternative to synthetic food preservatives based on eco-friendly and broad safety profile. Among various phytochemicals, aromatic plant essential oils (EOs) and their active components have been highly encouraged to be used as novel green preservative due to its considerable antibacterial, antifungal, antimycotoxigenic, insecticidal and antioxidant efficacy. Moreover, several EOs such as *Coriandrum sativum*, *Ocimum basilicum*, *Mentha piperita*, *Matricaria chamomilla*, *Cuminum cyminum* and EO bioactives such as limonene, carvone, eugenol, linalool, citral, vanillin, thymol and menthol are also grouped under generally recognized as safe category (GRAS), which strongly recommends botanical formulations as next generation pesticide (Prakash et al. 2018).

In spite of tremendous preservative potential, high volatility, less water solubility, intense aroma and easy degradation of active components limit the large scale practical application of EOs in food system (Marques et al. 2019). In order to deal with these challenges, nanoencapsulation of EOs using food grade biopolymer has emerged as a novel and efficient technique. In recent past, chitosan biopolymer has gained prime attention as superior encapsulating agent, based on its biodegradability, non-mammalian toxicity, hydrophilicity, controlled release and emulsion forming property (Wu and Liu 2008). Among different nanoencapsulation techniques utilized, ionic-gelation method is more preferred. This method is

comparatively simple, economical and non–toxic. Further, suitability for both hydrophilic and lipophilic component also suggests ionic-gelation method as an efficient strategy to formulate nanoemulsion.

Homalomena aromatica (Sugandh mantri) is an aromatic perennial herb reported for therapeutic values (Roy et al. 2019). *Homalomena aromatica* EO (HAEO) has been widely used in perfumery and cosmetics and reported to have potent antimicrobial efficacy (Policegoudra et al. 2012). However, the data are unavailable on the antiaflatoxigenic efficacy of HAEO and exploration of its preservative potential in food system. Moreover, no study has been performed on nanoencapsulation of HAEO in chitosan polymer. Hence, the present study focused on exploration of the efficacy of HAEO loaded chitosan nanoparticle as fungitoxic and antiaflatoxin B_1 candidate to prevent deterioration of spices under storage. Study comprised of biosynthesis of HAEO nanoparticle, its characterization, evaluation of antioxidant, antifungal and antimycotoxigenic efficacy along with probable mode of actions. The study also includes *in vivo* investigation on spice sample, sensorial analysis and assessment of lethal toxic dose in comparison with unencapsulated HAEO in order to strengthen recommendation as promising preservative agent in food sectors with sufficient consumer acceptance.

Methodology

Chemicals

Chemicals such as low molecular weight chitosan, glacial acetic acid, dichloromethane (DCM), tripolyphosphate (TPP), Tween 20, Tween 80, chloroform ($CHCl_3$), perchloric acid, nitric acid (HNO_3) methylglyoxal, diaminobenzene (DAB), thiobarbituric acid (TBA), trichloroacetic acid (TCA), potassium hydroxide (KOH), isoamyl alcohol, toluene, sucrose, acetonitrile, hydrochloric acid (HCl), n-heptane, methanol, sucrose, magnesium sulphate

115 ($MgSO_4$), potassium nitrate (KNO_3), yeast extract, DPPH and sodium chloride (NaCl) were
116 procured from SRL Pvt LTD and Hi-Media Mumbai, India.

117 **Test fungal species**

118 Aflatoxin secreting strain of *Aspergillus flavus* AF-LHP-NS 7 selected during mycobiota
119 analysis of different spices was utilized for further investigations. Storage fungi including
120 *Aspergillus niger*, *A. repens*, *A. luchuensis, A. terreus*, *Fusarium oxysporum*, *F. graminearum*,
121 *Penicillium italicum*, *P. chrysogenum*, *Mucor sp.*, *Rhizopus sp*., *Alternaria alternata*, *Curvularia*
122 *lunata* and Mycelia sterilia were used during fungitoxic experiments.

123 **Extraction and phytochemical analysis of HAEO**

124 Rhizomes of *Homalomena aromatica* procured from Varanasi, Uttar Pradesh, India, were
125 transferred to Clevenger's apparatus for 5 hour in order to extract EO.

126 Chemical characterization of HAEO was done through GC-MS analysis. TG-5 MS fused
127 silica capillary column of dimensions 30 m × 0.25 mm × 0.25 µm fitted inside Thermo Scientific
128 1300 GC interfaced with TSQ Duo triple quadruple mass spectrophotometer. Sample was
129 injected to column at 70 °C temperature with programmed increment up to 250 °C. Individual
130 phyto components were identified based on spectral peaks available in NIST, Wiley, and other
131 published literature (Carneiro et al. 2020).

132 **Synthesis of HAEO entrapped in chitosan based emulsion (CS-HAEO-Ne)**

133 CS-HAEO-Ne was prepared using ionic gelation technique (Rajkumar et al. 2020b). 1%
134 v/v glacial acetic acid (GAA) was added to 1.5% chitosan solution prepared in distilled water,
135 and mixed at 27 °C for 24 hour. Different w/v ratio of chitosan and HAEO *i.e.* 1:0, 1:0.2, 1:0.4,
136 1:0.6, 1:0.8 and 1:1 was prepared by mixing different amount of HAEO *i.e.* 0.00, 0.06, 0.12,
137 0.18, 0.24 and 0.30 g to chitosan solution. Further drop wise STPP (4 mg/mL) was added in

order to obtain nanoemulsion. Prepared nanoemulsion was lyophilized (Alpha 1-2 LD plus Entry Laboratory Freeze Drier for aqueous samples, John Morris Scientific, Sydney, Australia) at -62 °C for 72 hour and kept at 4 °C for further experiments.

Physico-chemical analysis of CS-HAEO-Ne

Structural and morphological analysis of lyophilized CS-Ne and CS-HAEO-Ne was performed through scanning electron microscopy (SEM) (EVO-18 researcher, Zeiss). A 10 fold dilution of 1 mg lyophilized CS-Ne and CS-HAEO-Ne was done followed by 10 min of sonication. A thin film of prepared solution was spreaded over glass slide, gold coated and viewed using SEM. Lyophilized CS-Ne and CS-HAEO-Ne was further used for FTIR analysis in between absorbance 500-4000 cm^{-1} at 4 cm^{-1}. Crystallinity of lyophilized CS-Ne and CS-HAEO-Ne was determined through XRD analysis using diffractometer at 2θ degree between 5-50°, step angle 0.02° min^{-1} with scan rate of 5° min^{-1}.

Estimation of nanoencapsulation efficiency (NEE) and loading capacity (LC)

Content of HAEO in CS-HAEO-Ne was estimated by UV-visible spectrophotometry. CS-HAEO-Ne (0.1 mL) was added in ethyl acetate (3 mL) followed by centrifugation at 10,000×g for 15 min. Content of HAEO was determined by taking the optical density of supernatant at absorbance maxima of HAEO *viz.* 265 nm and using calibration graph (R^2 = 0.998) of HAEO mixed in ethyl acetate. CS-Ne prepared in the same way was treated as control. NEE and LC were calculated through formula

$$\text{Nanoencapsulation efficiency(NEE)} = \frac{\text{Total amount of loaded HAEO} - \text{amount of HAEO into nanoemulsion}}{\text{Initial amount of HAEO}} \times 100$$

$$\text{Loading capacity(LC)} = \frac{\text{Mass of loaded HAEO}}{\text{Mass of loaded nanoemulsion}} \times 100$$

In vitro release profile of CS-HAEO-Ne

In vitro release profile of CS-HAEO-Ne was calculated following Chaudhari et al. (2020) with slight modification. 500 µL of CS-HAEO-Ne was added to 5 mL phosphate buffer saline (PBS and ethanol 3:2 v/v) under gentle agitation for 0-96 h at 30 °C. 3 mL suspension was removed at specific time interval which was replenished with the equal volume of fresh buffer. Amount of HAEO at each time was calculated by measuring absorbance at 293 nm as well as using standard calibration curve. Release profile of HAEO was calculated using the following formula.

$$\text{Cumulative release of HAEO (\%)} = \frac{\text{Cumulative amount of HAEO released at each time interval}}{\text{Initial mass of HAEO loaded in the sample}} \times 100$$

Antifungal and AFB_1 inhibitory efficacy of HAEO and CS-HAEO-Ne

Antifungal activity of HAEO and CS-HAEO-Ne was estimated as minimum inhibitory concentration (MIC). Toxigenic *A. flavus* AFLHP NS-7 strain was treated with different concentration of HAEO (0.25, 0.50, 0.75, 1.0, 1.25, 1.50 and 1.75 µL/mL) and CS-HAEO-Ne (0.25, 0.50, 0.75, 1.0, 1.25 µL/mL) for 10 days. Sample without any treatment worked as control. Minimum concentration of HAEO and CS-HAEO-Ne that completely inhibited growth of AFLHP NS-7 was considered as its MIC.

Antiaflatoxigenic efficacy of HAEO and CS-HAEO-Ne was calculated in terms of minimum aflatoxin inhibitory concentration (MAIC) (Rasooli and Abyaneh 2004). To determine the amount of AFB_1 content, filtered media was extracted with chloroform and developed in TLC plate by using mobile phase toluene, isoamyl alcohol and methanol in 90:32:2 (v/v/v).

Absorbance of spots was recorded at 360 nm and AFB_1 content was calculated based on the formula given below.

$$AFB_1\ (\mu g/mL) = \frac{\text{Absorbance at 360 nm} \times \text{Molecular weight of } AFB_1}{\text{Molar extinction coefficient of } AFB_1 \times \text{Path length}} \times 1000$$

Where, molecular mass of AFB_1 is 312 g/mol, molar extinction coefficient is 21800 mol cm^{-1} and path length is 1 cm.

% inhibition of AFB_1 was calculated as

$$\%\ \text{inhibition} = \frac{AFB_1\ (\text{control}) - AFB_1(\text{treatment})}{AFB_1\ (\text{control})} \times 100$$

Antifungal action of HAEO and CS-HAEO-Ne

Ergosterol quantification

In order to estimate ergosterol content of fungal plasma membrane, *A. flavus* cells were treated with different concentration of HAEO *and* CS-HAEO-Ne (0.25, 0.50, 0.75, 1.0, 1.25 and 0.25, 0.50 and 0.75 µL/mL, respectively) and kept in B.O.D. incubator for 5 days at 27 ± 2 °C. Samples without HAEO and CS-HAEO-Ne worked as controls. *A. flavus* biomass was harvested from each sample and net wet weights of mycelia were measured followed by vortexing in 25% KOH solution. Thereafter, ergosterol from samples was extracted using n-heptane and water 2:5 (v/v) and scanned spectrophotometrically between 230-300 nm. Formula given by Tian et al. (2012) was used to quantify ergosterol.

% egrosterol+ % 24 (28) dehydroergosterol= (A_{282}/ 290)/ Pellet weight

% 24 (28) dehydroergosterol= (A_{230}/ 518)/ Pellet weight

% egrosterol= (% egrosterol+ % 24 (28) dehydroergosterol) - % 24 (28) dehydroergosterol

Where 290 and 518 are the E values determined for crystalline ergosterol and dehydroergosterol, respectively.

Effect on cellular cations (Ca^{2+}, K^+ and Mg^{2+}) and 260 and 280 absorbing materials

Seven days grown biomass of *A. flavus* obtained from liquid SMKY media was fumigated HAEO (0.25 to 1.75 µL/mL and 2 MIC) and CS-HAEO-Ne (0.25 to 1.25 µL/mL and 2 MIC). Efflux of calcium, potassium and magnesium ions was analyzed by atomic absorption spectroscopy (Perkin Elmer AAnalyst 800, USA). For measuring release of 260 and 280 nm absorbing materials, 7 days grown *A. flavus* biomass was treated with different concentration of HAEO and CS-HAEO-Ne *i.e.,* 0.25 to 1.75 µL/mL and 0.25 to 1.25 µL/mL as well as 2 MIC doses, respectively for 24 h and absorbance of samples were taken at 260 and 280 nm.

HAEO and CS-HAEO-Ne effect on methylglyoxal (MG)

Seven days old *A. flavus* mycelia was treated at different doses *viz.* MIC and 2MIC (1.75 and 3.5 µL/mL) of HAEO and MIC and 2MIC (1.25 to 2.5 µL/mL) of CS-HAEO-Ne for 24 h. Samples without HAEO and CS-HAEO-Ne were treated as controls. Estimation of methyglyoxal was done following the methods of Yadav et al. (2005). 300 mg sample from each set was crushed in 3 mL of perchloric acid (0.5 M) and subjected to centrifugation at 4 °C on 10000 x g for 10 min. Supernatant was neutralized (pH = 7) by saturated potassium carbonate solution and centrifuged again at 10000 x g for 10 min (4 °C). Reaction mixture containing 0.5 mL 1,2 diaminobenzene (DAB), 0.2 mL $HClO_4$ (5 M) and 1.3 mL neutralized supernatant was prepared and its optical density was recorded at 341 nm. Total amount of MG was estimated using the standard curve of pure MG (10-100 µM).

Antioxidant potential of HAEO, CS-Ne and CS-HAEO-Ne

Free radical removal potential of HAEO, CS-Ne and CS-HAEO-Ne was calculated using the DPPH assay following slightly modified method of Balasubramani et al. (2017). IC_{50} (50 % radical scavenging potential of HAEO, CS-Ne and CS-HAEO-Ne) was determined using the following formula

% Radical scavenging potential = $(A_0-A_1)/A_0 \times 100$

Where A_0 and A_1 are expressing the absorbance of blank and samples (HAEO, CS-Ne and CS-HAEO-Ne) at 517 nm, respectively.

Estimation of phenolics present in HAEO, CS-Ne and CS-HAEO-Ne

Amount of phenolics in HAEO, CS-Ne and CS-HAEO-Ne was calculated following Dzhanfezova et al. (2020) with slight modifications. Reaction mixture containing Folin-Ciocalteu's reagent and sample was allowed to stand for 2 h in dark after addition of 3 mL Na_2CO_3 and optical densities of samples were measured at 760 nm. The result was calculated in terms of µg gallic acid equivalent (GAE)/g.

$$\text{Absorbance (760 nm)} = 0.0012 \times \text{GA (µg)} + 0.024$$

Study on in vivo AFB_1 inhibitory efficacy of HAEO and CS-HAEO-Ne in (*Nigella sativa*) food system: High performance liquid chromatography (HPLC) assay

In situ efficacy of HAEO and CS-HAEO-Ne were estimated by fumigating black cumin seeds (model spice system; 250 g) in 500 mL air tight plastic containers for storage period of 18 months. Spice samples were fumigated with HAEO and CS-HAEO-Ne at their respective MIC concentrations. Control sets were devoid of any treatment.

AFB_1 content in stored spice samples were determined through HPLC method following Sheijooni-Fumani et al. (2011). 5 g of grinded spice samples were mixed with methanol and double distilled water (8/10; v/v), centrifuged and supernatant was mixed with 300 µL chloroform and 6 mL water containing 3% KBr. Obtained reaction mixtures were centrifuged again (5000 x g), settled portion was isolated and dried at 85 °C on water bath and further dissolved in 500 µL of HPLC grade methanol for injecting into HPLC column. Amount of AFB_1 (µg/kg) was determined at 365 nm from the prepared standard curve of AFB_1 (50-500 ng/50 µL)

(Upadhyay et al. 2018). Methanol, acetonitrile and water (17:19:64 v/v/v) was used as mobile phase (1.2 mL/min flow rate) to separate AFB_1 on C18 reverse phase column (4.6 mm × 25 cm × 5 µm) at ambient temperature of 25 °C.

Analysis of lipid peroxidation and mineral loss in HAEO and CS-HAEO-Ne treated black cumin (*Nigella sativa*) seeds

In vivo preservative efficacy of HAEO and CS-HAEO-Ne was tested in terms of lipid peroxidation inhibitory action at their respective MIC and 2 MIC value following Iseri et al. (2013). Lipid peroxidation was measured using thiobarbituric acid reactive substance (TBRAS) assay. In order to execute experiment, 1 g of grinded spice sample was added to 5 mL TBA reagent comprising 0.375 % TBA, 15 % TCA, and 0.2 N HCl. Further, samples were subjected to water bath at 95 °C for 25 min, following centrifugation (10000 x g for 10 min). Thereafter, absorbance of supernatant was recorded at 532 nm and 600 nm and results were expressed as µM equivalent MDA/g FW. Mineral biodeterioration level in HAEO and CS-HAEO-Ne treated spice samples were evaluated through atomic absorption spectrometry (Perkin Elmer AAnalyst 800, USA).

Sensorial analysis of fumigated black cumin (*Nigella sativa*) seeds with HAEO and CS-HAEO-Ne

Effect of HAEO and CS-HAEO-Ne fumigation (at MIC concentration) on sensorial characteristics of stored black cumin seeds (18 months duration) was analyzed by a panel comprising of 10 panelists of both genders. 7 point hedonic scale (5 = extremely like, 4 = slightly like, 3 = neither like nor dislike, 2 = slightly dislike, 1 = extremely dislike) was used to estimate taste, colour and odor of stored spice samples.

Safety profile assessment of HAEO and CS-HAEO-Ne

Safety profile of HAEO and CS-HAEO-Ne was evaluated in terms of toxicity assay on male mice using oral administration and represented in terms of LD_{50} value (Singh et al. 2020b). Different amount of HAEO and CS-HAEO-Ne mixed with stock solution (Tween 20 and deionized distilled water, 1:1) were administered orally to each mice group (10 mice). Mice administered with stock and CS-Ne was considered as control. LD_{50} value was based on the number of mice dead within 24 h of study period and calculated through probit analysis.

Statistical analysis

The experiments were carried out in triple sets and the data represented as mean (n = 3) ± standard error (SE). Further it was analyzed by one way ANOVA followed by Tukey's B multiple comparison test at significant ($P < 0.05$) differences. SPSS and Sigma plot program were used for data analysis and creating graphs.

Result and discussion

Extraction and GC-MS of HAEO

HAEO was extracted from rhizome of the plant and per cent yield was found to be 8.6 mL/kg. Phytochemical analysis of HAEO through GC-MS analysis revealed 26 compounds comprising 91.71% of EO. Linalool was found to be the major component contributing 68.51% of total bioactive components. The outcomes of the present study are in line with the previous study of Policegoudra et al. (2012) describing linalool (62.5%) as the major bioactive component. Per cent occurrence and retention time of different compounds are presented in Table 1. Bioefficacy of EOs are based on their bioactive components whose composition and amount may vary with variation in geological and environmental conditions, harvesting stage and oil extraction procedure, ultimately affecting the biological activity of EOs (Dhifi et al.

296 2016). Thus, analysis of EO bioactive composition is a crucial step before its detailed bioactivity
297 evaluation.

298 Preparation of HAEO loaded chitosan nanoemulsion (CS-HAEO-Ne)

299 CS-HAEO-Ne was prepared using tripolyphasphae (TPP) as cross linking agent
300 following ionic gelation technique. Interaction between protonated -NH_2 group of chitosan and
301 negative charged ions of TTP leads to formation of biocompatible nanoparticles. CS-HAEO-Ne
302 was formed following the two step strategy *i.e.* droplet formation and solidification.

303 Encapsulation enhance stability of volatile aromatic substances such as EOs and their
304 bioactive components against environmental factors *i.e.* light, chemical, oxygen, pressure and
305 heat mediated degradation (Delshadi et al. 2020). Ionotropic gelation method is well known for
306 encapsulating bioactive principles due to its non toxic, organic solvent free, appropriate and
307 easily controllable properties (Esmaeili and Asgari 2015). Chitosan, obtained by deacetylation of
308 chitin, was selected as coating matrix as it an efficient, non toxic, biodegradable and film/ gel
309 forming polymer matrix. Effective entrapment of HAEO was determined through preparing
310 different chitosan and HAEO ratios *viz.* 1:0, 1:0.2, 1:0.4, 1:0.6, 1:0.8 and 1:1.

311 Physico-chemical characterization of CS-HAEO-Ne

312 Scanning electron microscopic (SEM) analysis

313 SEM analysis was done to analyze the morphological features of CS-Ne and CS-HAEO-
314 Ne which depicted spherical structure and smooth surface of the prepared nanoparticles. Size of
315 CS-Ne and CS-HAEO-Ne was found in range of 37-81.4 nm and 48.3-94.6 nm, respectively
316 (Fig. 1A, 1B). Increment in size of CS-Ne after encapsulation of HAEO could be to the result of
317 swelling of chitosan matrix by entrapped HAEO (Kumar et al. 2019). This finding on enhanced

particle size of EO loaded nanoparticles in comparison to unencapsulated chitosan nanoparticle is supported by previous reports of Hosseini et al. (2013).

Fourier transform infrared (FTIR) spectroscopic analysis

FTIR analysis of pure chitosan powder, CS-Ne, HAEO and CS-HAEO-Ne showing chemical interaction between chitosan and HAEO are presented in Fig. 2. Chitosan indicated specified peaks at 3445 cm^{-1} for -OH and -NH stretching, 2916 cm^{-1} for symmetric or asymmetric –CH stretching and at 1066 cm^{-1} for C-O-C linkage. In addition 1645 cm^{-1}, 1581 cm^{-1} and 1316 cm^{-1} peaks represented presence of amide I, amide II and amide III group (Branca et al. 2016). Prominent peak at 1375 cm^{-1} in chitosan represent –C-N- bond stretching. Presence of new peaks in CS-Ne at 1556 cm^{-1} (N-H bending) and 888 cm^{-1} (P-O stretching) specified the electrostatic bonding between amide group of CS and phosphate moiety of TPP. Furthermore, in HAEO several peaks at/in between 1644-1447cm^{-1} (for phenyl ring), 1713 cm^{-1} for presence of ether group, 3541 cm^{-1} (O-H stretching), 2966 cm^{-1} (–CH stretching) and 739 cm^{-1} (aromatic C-H bending) appeared. Most of the aforementioned peaks were retained in the spectra of CS-HAEO-Ne. Shifting of peak from 2966 cm^{-1} in spectra of HAEO to 2922cm^{-1} in spectra of CS-HAEO-Ne also denotes successful encapsulation of HAEO inside chitosan polymer.

X-ray diffraction (XRD) analysis

Crystallographic pattern of chitosan powder, CS-Ne and CS-HAEO-Ne has been shown in Fig. 3. Diffraction spectrum of chitosan powder represented peaks at 2θ value 10.2° and 19.8°, denoting the characteristic peak of chitosan *viz.* 10° and 20° and increased crystallinity (Su et al. 2020). However, the diffractogram of CS-Ne and CS-HAEO-Ne depicted flattening and broadening of characteristic peaks suggesting destruction of chitosan crytallinity as a result of successful TPP cross linking with chitosan and loading of HAEO into the polymer matrix.

Estimation of per cent nanoencapsulation efficiency (NEE) and loading capacity (LC) of CS-HAEO-Ne

NEE and LC of HAEO inside chitosan nanomatrix was determined through UV-visible spectrophotometric analysis which revealed that NEE and LC of CS-HAEO-Ne ranged between 22.0-83.41 % and 0.15-2.32 % (Table 2). NEE showed dose dependent increment up to the ratio 1:1.08 (CS:HAEO), representing good entrapment of HAEO inside chitosan nanomatrix. However, decline in NEE was recorded at the ratio 1:1 (CS: HAEO) depicting insufficiency of chitosan matrix to entrap further more HAEO. The result is in accordance with the previous reports of Feyzioglu and Tornuk (2016).

In vitro release of CS-HAEO-Ne

The *in vitro* cumulative release mechanism of HAEO from CS-HAEO-Ne was measured at room temperature for 1:0.8 ratio of chitosan to HAEO. The release of EO comprised of two steps *i.e.* initial rapid release and then constant release as shown in Fig. 4. This result is supported by the previous study of Li et al. (2018) describing controlled release of curcumin encapsulated in chitosan. Initial fast release phase could be a response of unencapsulated EO that is adsorbed on the surface of polymeric matrix or due to diffusion of EO from higher concentration till attainment of equilibrium. After 6 h, release was recorded to be 51.36 % followed by 26.90 % and 3.27 % release in between (10-24) and (24-96) h respectively. Maximum release of EO observed was 81.55 % after 96 h, showing that 1.87 % HAEO out of 83.41 % was still entrapped inside the polymeric matrix. The result suggested that encapsulation maintained the stability of volatile compounds through its control release.

In vitro antifungal and antiaflatoxigenic efficacy of HAEO and CS-HAEO-Ne

Minimum inhibitory concentration (MIC) and AFB_1 inhibitory concentration of HAEO was 1.75 µL/mL and 1.25 µL/mL, respectively. However, CS-HAEO-Ne showed enhanced the bioefficacy against *A. flavus* and its MIC and MAIC value declined to 1.25 µL/mL and 1.0 µL/mL, respectively (Table 3). In addition, both HAEO and CS-HAEO-Ne significantly suppressed the growth of other storage molds (*A. niger*, *A. repens, A. luchuensis, A. terreus*, *Fusarium oxysporum*, *F. graminearum*, *Penicillium italicum*, *Mucor sp., Rhizopus sp., P. chrysogenum Alternaria alternata, Curvularia lunata* and Mycelia sterilia) at their respective MIC values *viz.,* 1.75 µL/mL and 1.25 µL/mL (Fig. 5). Potent fungitoxic profile of HAEO and its nanoformulation also favored for their application as botanical preservative for stored products. The boosted bio-efficacy of CS-HAEO-Ne in comparison to HAEO could be the result of controlled release and improved stability of constituent volatiles, enhanced water solubility, wider surface area and fastened adsorption through cell wall and membrane (Hasheminejad et al. 2019). The antifungal efficacy of HAEO is more efficacious than other reported EOs such as *Pelargonium roseum* EO (3.8 µL/mL), *Thymus vulgaris* EO (2.3 µL/mL) and *Cymbopogon nardus* EO (6.4 µL/mL) (Zabka et al. 2009) and other synthetic preservatives such as propionic acid and sodium sulphite having MIC value ranged from 2 to > 83 µL/mL against *P. verrucosum* and two strain of *A. westerdikiae* (Schlosser and Prange 2018). The boosted potency of encapsulated HAEO could also be due to additive action of chitosan and HAEO. Cationic charge of chitosan has been reported to interact with anionic charges of oxygenated lactone ring causing enhanced antiaflatoxigenic efficacy (Cortes-Higareda et al. 2019). Hence, CS-HAEO-Ne could be highly preferred green preservative over other synthetic preservatives with potent toxicity.

Antifungal mode of action of HAEO and CS-HAEO Ne

Effect on ergosterol content and leakage of vital cellular ions

Ergosterol is the unique sterol associated with fungal plasma membrane, responsible to maintain proper functioning of membrane by controlling membrane permeability and integrity. Ergosterol content in treated *A. flavus* cells declined in dose dependent manner with increasing doses of 0.25, 0.50, 0.75, 1.0 and 1.25 µL/mL. HAEO concentrations showed 33.96 %, 40.78 %, 46.81 %, 61.91 % and 82.31 % decline of ergosterol content, respectively. However, CS-HAEO-Ne inhibited ergosterol content to 11.02 %, 33.26 % and 96.88% at just 0.25, 0.50 and 0.75 µL/mL respectively (Fig. 6). Obtained results are supported by the investigations of Khan et al. (2010). Antifungal drugs such as azoles are reported to inhibit ergosterol biosynthesis through targeting cytochrome 450 lanosterol 14α-demethylase enzyme, the ERG11 gene product involved in ergosterol pathway (Lupetti et al. 2002). Thus, HAEO and CS-HAEO-Ne mediated depletion in ergosterol content could also be based on downregulation of lanosterol 14α demethylase enzyme functioning, involved in crucial step of ergosterol biosynthesis *i.e.* 14α demethylation. Decline of ergosterol content would make membrane porous leading to loss of vital ions *viz.* Ca^{+2}, Mg^{+2} and K^{+} as well as 260 nm and 280 nm absorbing material (Table 4), responsible for vital metabolic activities of cell. Therefore, present study concluded fungal plasma membrane as one of the prime targets for antifungal action of HAEO and CS-HAEO-Ne as the cause of cell death through altering vital cellular mechanisms of fungus.

Methylglyoxal (MG), an endogeneous product of metabolic pathways such as polyol pathway, glycolytic pathway and amino acetone metabolism is reported to be highly reactive and strong glycaling agent (Antognelli et al. 2013). MG is also reported to induce cytotoxic effects through inducing apoptosis *via* enhancing reactive oxygen species production or through accumulation of MG mediated advanced glycation end products. Moreover, MG has been also reported to have inductive role in AFB_1 production. Chen et al. (2004) reported upregulation of

409 the major regulatory gene *aflR* and other AFB_1 biosynthetic gene *nor1* by MG. In present
410 experiment MG content in control was found to be 232.4 μM/g FW, while it decreased in HAEO
411 treated cells in dose dependent manner. Further, CS-HAEO-Ne depicted maximum suppression
412 of MG formation in treated cells at relatively low concentration in comparison to unencapsulated
413 HAEO (Fig. 7). Obtained outcome is in accordance with the findings of Chaudhari et al. (2020).
414 Considerable difference between bioactivity of unencapsulated and encapsulated HAEO might
415 be due to enhanced bioavailability along with targeted and slow release caused by encapsulation.
416 Based on the above findings, we hypothesize that inhibition of MG formation might have a
417 significant role in antiaflatoxigenic activity of HAEO or CS-HAEO-Ne.

418 **Antioxidant efficacy**

419 DPPH based free radical scavenging assay basically relies on the principle of antioxidant
420 mediated quenching of single electron form DPPH radical and subsequently decolorization of
421 purple colour of DPPH solution. Encapsulation of EOs along with boosting its bioefficacy also
422 enhances its antioxidant potency through protecting bioactive components of EOs from
423 environmental degradation caused due to light and temperature. In the present experiment CS-
424 HAEO-Ne depicted enhanced antioxidant potency over HAEO. IC_{50} value for HAEO and CS-
425 HAEO-Ne were recorded as 15.98 μL/mL and 4.57 μL/mL, respectively, describing
426 enhancement of antioxidant potency through nanoencapsulation (Fig. 8). In addition, chitosan
427 was found to be deprived of promising antioxidant efficacy. Siva et al. (2020) also reported
428 enhanced antioxidant efficacy of isoeugenol encapsulated inside methyl β-cyclodextrin in
429 comparison to its free form. In addition, Cetin Babaoglu et al. (2017) suggested that boosted free
430 radical scavenging potency of hydropropyl beta cyclodextrin (HPβCD) loaded clove EO was
431 either due to its enhanced water solubility or preservation of phenolic compounds under Clove-

HPβCD complex from oxidative degradation. IC_{50} value of CS-HAEO-Ne is lower in comparison to that recorded for other synthetic antioxidants as ascorbic acid and BHT (Ricci et al. 2005), suggesting encapsulated HAEO as future sustainable green food preservative.

Total phenolic content of chitosan, HAEO and CS-HAEO-Ne was found as 0.18 (µg gallic acid equivalent/g HAEO), 3.37 and 5.91 µg gallic acid equivalent respectively. The present result showed improved total phenolic content of HAEO after encapsulation which is in accordance with the previous study of Attallah et al. (2020). Such enhancement could result due to enhanced surface to volume ratio of nanomeric particle size of EO. In addition, ameliorated water solubility of EO phenolic content as well as its improved protection against evaporation loss by environmental gradient also contributes towards enhanced total phenolics.

In situ antifungal and antiaflatoxigenic potential of HAEO and CS-HAEO Ne on black cumin seeds (model food system)

Based on *in vitro* investigations, HAEO and CS-HAEO-Ne was found to be efficient antifungal and antiaflatoxigenic agent. However, in order to recommend large scale commercialization, it is mandatory to analyze *in situ* efficacy. HPLC analysis of 18 months stored black cumin seed sample manifested potent AFB_1 inhibitory efficacy of HAEO and CS-HAEO-Ne. HPLC result depicted 208.37 µg/Kg concentration of AFB_1 in control samples. While both HAEO and CS-HAEO-Ne completely inhibited AFB_1 biosynthesis at their respective MIC concentrations. AFB_1 concentration at MIC of both HAEO and CS-HAEO-Ne was found to be 7.39 µg/Kg and 7.34 µg/Kg (Fig. 9). Highly efficacious *in situ* antifungal and antiaflatoxigenic potency of non-encapsulated as well as encapsulated HAEO is based on its diverse *in vitro* antifungal mode of actions such as disruption of membrane permeability through

depleting ergosterol content, leakage of vital cellular components and ions as well as through inhibiting biosynthesis of aflatoxin inducer molecule (methylglyoxal).

Estimation of lipid peroxidation inhibitory efficacy and mineral preservation potency of HAEO and CS-HAEO-Ne fumigated *Nigella sativa* seeds

Reactive oxygen species (ROS) like superoxide radical and peroxide radicals due to its highly reactive nature interact with biomolecules such as nucleic acids, proteins and polyunsaturated fatty acids (PUFAs). Reaction between ROS and PUFA ultimately leads to generation of malondialdehyde (MDA), F_2-isoprostanes and 4-hydrox-2-nonenal (HNE), a biomarker molecule of oxidative stress or lipid peroxidation (Tsikas 2017). The MDA, a significant biomarker of lipid peroxidation, generate pink colour MDA-thiobarbituric acid complex which is measured via TBARS assay in order to quantify lipid peroxidation in a sample. In control sets for HAEO and CS-HAEO Ne MDA content was noted as 351.21 and 334.39 µM/g FW. However, MDA content in HAEO treated samples was declined and found to be 224.51 and 129.03 µM/g FW at its MIC and 2 MIC value, respectively. Conversely, samples fumigated with encapsulated HAEO revealed presence of only 176.8 and 105.8 µM/g FW MDA content at relatively low concentration (Fig. 10). Outcome of the result is corroborated with the previous report of Hu et al. (2015) suggesting enhanced preservative potential of cinnamon essential oil loaded chitosan nanoparticle in order to prevent lipid peroxidation and maintain sensory quality of stored meat based on synergism between antioxidant potency of HAEO and chitosan. Moreover, earlier reported resistance quality of chitosan coating towards oxygen permeability and of chitosan amine group with malondialdehyde (Sathivel et al. 2007) might also be one of the major causes related with boosting of preservative potential of nanoencapsulated EO. Furthermore, entrapped HAEO inside chitosan matrix have been protected against environmental degradation, have

sustainable release profile and potent free radical scavenging property might be a promising reason owing to its shelf life enhancer efficacy. Mineral content of stored food substances are also lost due to action of storage fungi. Fagbohun and Ogundahunsi (2019) reported diminished mineral content in stored *Citrullus lanatus* seeds, as the minerals are metabolized and utilized by the storage fungi for their growth and physiological activity. Black cumin seed is reported to have vast medicinal history and it is huge repository of nutritional substances and minerals such as iron, sodium, potassium, phosphorus, calcium, manganese, zinc, magnesium, and copper. Our experimental analysis revealed that fumigation of HAEO as well as CS-NHAEO-Ne has capability to preserve nutritional property of black cumin via protecting its mineral content loss. Table 5 presents mineral content in control, HAEO and CS-NHAEO-Ne fumigated black cumin seed at its MIC and 2 MIC concentrations. Hence, the present investigation recommends CS-NHAEO to be used as a sustainable green shelf life enhancer food additive substance.

Sensorial profile of black cumin (*Nigella sativa*) seeds fumigated with HAEO and CS-HAEO-Ne

Sensorial properties of food products are important perspective with respect to consumer's acceptance. Therefore, in order to recommend HAEO loaded nanoformulation as commercial green food preservative, it is a very crucial to evaluate sensorial attributes of fumigated samples for its wide consumer acceptance in global market. Considering this, three different sets of 18 months stored samples *i.e.* stored black cumin seed without fumigation, black cumin seed fumigated with HAEO at MIC concentration *i.e.*1.75 µL/ml and black cumin seed fumigated with CS-HAEO-Ne at its MIC concentration *i.e.*1.25 µL/ml sensorial aspects was assessed. Obtained result is presented in Fig. 11. The obtained sensorial score for odor, taste, texture and colour was lower for control set, in comparison to fumigated samples. However, in between

HAEO and CS-HAEO-Ne treated samples CS-HAEO-Ne is having better score suggesting food grade coating as an efficient strategy to prevent undesirable sensorial effect of HAEO on food products. Entrapment of HAEO inside polymeric nanomatrix masked the intense aroma of essential oil and caused its controlled release as well as lower concentration of EO is required; besides, above mentioned potent radical scavenging action, prevention of lipid peroxidation and efficient antifungal characteristics of encapsulated HAEO also contributed to its food items sensorial properties preservation quality. Pabast et al. (2018) reported nanoencapsulated *Satureja khuzestanica* EO as better substance over free EO to extend shelf life of lamb meat with improved sensorial quality.

Safety assessment of HAEO and CS-HAEO-Ne: Acute oral toxicity test on male mice

In acute oral toxicity assay, LD_{50} value for HAEO was determined as 11334.6 µL/kg body weight, while it is 8006.84 µL/kg for CS-HAEO-Ne. Controls containing Tween 20 and chitosan nanoemulsion are non toxic to the mice. The outcome is in accordance with the previous report of Ribeiro et al. (2014), indicating that encapsulated *Eucalyptus citriodora* EO have enhanced acute oral toxicity in comparison to free EO. LD_{50} value of HAEO was higher as compared to some previous studies focused on plant products like *Nepeta cataria* EO *i.e*. 2710 mg/kg BW (Zhu et al. 2009), *Artemisia annua i.e.* 790 mg/kg (Perazzo et al. 2003), thymol and carvacrol bioactive component *i.e.* 980 mg/kg and 810 mg/kg (Bahuguna et al. 2020) recommending nanoformulated HAEO as safer next generation green preservative.

Conclusion

The findings of present study recommend utilization of nanoformulated essential oils as efficacious antifungal agent. Encapsulated HAEO exhibited improved antifungal,

antiaflatoxigenic as well as free radical scavenging activity over the unencapsulated HAEO. Noticeable destruction of ergosterol level, efflux of important cellular ions and inhibition of methylglyoxal biosynthesis suggested possible mechanisms underlying antifungal and AFB_1 suppression potencies of encapsulated HAEO. Moreover, CS-HAEO Ne was also found to have significant *in vivo* AFB_1 inhibitory potency as well as protective role against lipid peroxidation and mineral loss in stored *Nigella sativa* seeds without compromising its organoleptic attributes. Thus, the above findings provide an exciting future opportunity for food industries to prefer HAEO nanoformulation as a natural and safe alternative of synthetic chemicals due to its potent preservative potential and safety profile.

Author contribution

Shikha Tiwari: Conceptualization, writing-original review draft, funding acquisition; Neha Upadhyay: Review and editing; formal analysis; Bijendra Kumar Singh: Experimental analysis; Vipin Kumar Singh: Review and editing, data curation; Nawal Kishore Dubey: writing–review and editing, supervision. All authors have reviewed and approved the final manuscript.

Funding

This study was supported by the University Grant Commission (UGC) [grant no.: 16-9(June 2018)/2019(NET/CSIR)], New Delhi, India.

Data availability

All data analysed during this study are included in this manuscript.

Declarations

Ethics approval

The animal based experiment was performed according to the ethical standards of the institution.

Consent to participate

All authors participated in this work.

Consent for publication

All authors agree to publish this article in the Environmental Science and Pollution Research.

Conflict of interest

Authors declare that they have no competing interests.

References

Antognelli C, Mezzasoma L, Fettucciari K, Talesa VN (2013) A novel mechanism of methylglyoxal cytotoxicity in prostate cancer cells. Int J Biochem Cell Biol 45:836-844.

Attallah OA, Shetta A, Elshishiny F, Mamdouh W (2020) Essential oil loaded pectin/chitosan nanoparticles preparation and optimization *via* Box–Behnken design against MCF-7 breast cancer cell lines. RSC Advances 10:8703-8708.

Bahuguna A, Ramalingam S, Arumugam A, Natarajan D, Kim M (2020) Molecular and *in silico* evidences explain the anti-inflammatory effect of *Trachyspermum ammi* essential oil in lipopolysaccharide induced macrophages. Process Biochem 96:138-145.

Balasubramani S, Rajendhiran T, Moola AK, Diana RKB (2017) Development of nanoemulsion from *Vitex negundo* L. essential oil and their efficacy of antioxidant, antimicrobial and larvicidal activities (*Aedes aegypti* L.). Environ Sci Pollut Res 24:15125-15133.

Branca, C., D'Angelo, G., Crupi, C., Khouzami, K., Rifici, S., Ruello, G., & Wanderlingh, U. (2016). Role of the OH and NH vibrational groups in polysaccharide-nanocomposite interactions: A FTIR-ATR study on chitosan and chitosan/clay films. Polymer 99:614-622.

567 Carneiro JNP, da Cruz RP, Campina FF, do Socorro Costa M, Dos Santos ATL, Sales DL,
568 Bezerra CF, da Silva LE, de Araujo JP, do Amaral W, Rebelo RA, Begnini IM, de Lima
569 LF, Coutinho DM, Morais-Braga MFB (2020) GC/MS analysis and antimicrobial activity
570 of the *Piper mikanianum* (Kunth) Steud. essential oil. Food Chem Toxicol 135:1-8.

571 Cetin Babaoglu H, Bayrak A, Ozdemir N, Ozgun N (2017) Encapsulation of clove essential oil
572 in hydroxypropyl beta-cyclodextrin for characterization, controlled release, and
573 antioxidant activity. J Food Process Preserv 41:1-8.

574 Chaudhari AK, Singh VK, Das S, Prasad J, Dwivedy AK, Dubey NK (2020) Improvement of *in*
575 *vitro* and *in situ* antifungal, AFB_1 inhibitory and antioxidant activity of *Origanum*
576 *majorana* L. essential oil through nanoemulsion and recommending as novel food
577 preservative. Food ChemToxicol 143:1-12.

578 Chen ZY, Brown RL, Damann KE, Cleveland TE (2004) Identification of a maize kernel stress-
579 related protein and its effect on aflatoxin accumulation. Phytopathology 94:938-945.

580 Cortes-Higareda M, de Lorena Ramos-Garcia M, Correa-Pacheco ZN, Del Rio-Garcia JC,
581 Bautista-Banos S (2019) Nanostructured chitosan/propolis formulations: characterization
582 and effect on the growth of *Aspergillus flavus* and production of aflatoxins. Heliyon 5:1-
583 7.

584 Delshadi R, Bahrami A, Tafti AG, Barba FJ, Williams LL (2020) Micro and nano-encapsulation
585 of vegetable and essential oils to develop functional food products with improved
586 nutritional profiles. Trends Food Sci Technol 104:72-83.

587 Dhifi W, Bellili S, Jazi S, Bahloul N, Mnif W (2016) Essential oils' chemical characterization
588 and investigation of some biological activities: A critical review. Medicines 3:1-16.

589 Dzhanfezova T, Barba-Espin G, Muller R, Joernsgaard B, Hegelund JN, Madsen B, Larsen DH,
590 Vega MM, Toldam-Andersen TB (2020) Anthocyanin profile, antioxidant activity and
591 total phenolic content of a strawberry (Fragaria× ananassa Duch) genetic resource
592 collection. Food Biosci 36:1-7.

593 Esmaeili A, Asgari A (2015) *In vitro* release and biological activities of *Carum copticum*
594 essential oil (CEO) loaded chitosan nanoparticles. Int J Biol Macromol 81:283-290.

595 Fagbohun E, Ogundahunsi AS (2019) Effects of storage on nutritional, mineral composition and
596 mycoflora of stored sundried *Citrullus lanatus* Thunberg (Melon) seeds. Int J Biochem
597 Res Rev 28:1-7.

598 Feyzioglu GC, Tornuk F (2016) Development of chitosan nanoparticles loaded with summer
599 savory (*Satureja hortensis* L.) essential oil for antimicrobial and antioxidant delivery
600 applications. LWT- Food Sci Technol 70:104-110.

601 Food and Agriculture organization (FAO, 2004). Regulations for mycotoxins in food and feed in
602 2003. FAO, Food and Nutrition, paper 81. FAO, Rome, Italy.

603 Gupta M (2010) Pharmacological properties and traditional therapeutic uses of important Indian
604 spices: A review. Int J Food Prop 13:1092-1116.

605 Hasheminejad N, Khodaiyan F, Safari M (2019) Improving the antifungal activity of clove
606 essential oil encapsulated by chitosan nanoparticles. Food Chem 275:113-122.

607 Hosseini SF, Zandi M, Rezaei M, Farahmandghavi F (2013) Two-step method for encapsulation
608 of oregano essential oil in chitosan nanoparticles: preparation, characterization and *in*
609 *vitro* release study. Carbohydr Polym 95:50-56.

610 Hu J, Wang X, Xiao Z, Bi W (2015) Effect of chitosan nanoparticles loaded with cinnamon
611 essential oil on the quality of chilled pork. LWT-Food Sci Technol 63:519-526.

612 International agency for research on cancer (IARC) (2012) Chemical agents and related
613 occupations. IARC monographs on the evaluation of carcinogenic risks to humans,
614 Volume 100F.

615 Iseri OD, Korpe DA, Sahin FI, Haberal M (2013) Hydrogen peroxide pretreatment of roots
616 enhanced oxidative stress response of tomato under cold stress. Acta Physiol
617 Plant 35:1905-1913.

618 Khan A, Ahmad A, Akhtar F, Yousuf S, Xess I, Khan LA, Manzoor N (2010) *Ocimum sanctum*
619 essential oil and its active principles exert their antifungal activity by disrupting
620 ergosterol biosynthesis and membrane integrity. Res Microbiol 161:816-823.

621 Kovesi B, Cserhati M, Erdelyi M, Zandoki E, Mezes M, Balogh K (2020) Lack of dose-and
622 time-dependent effects of aflatoxin b_1 on gene expression and enzymes associated with
623 lipid peroxidation and the glutathione redox system in chicken. Toxins 12:1-11.

624 Kumar A, Kujur A, Singh PP, Prakash B (2019) Nanoencapsulated plant-based bioactive
625 formulation against food-borne molds and aflatoxin B1 contamination: Preparation,
626 characterization and stability evaluation in the food system. Food Chem 287:139-150.

627 Li MF, Chen L, Xu MZ, Zhang JL, Wang Q, Zeng QZ, Wei XC, Yuan Y (2018) The formation
628 of zein-chitosan complex coacervated particles: Relationship to encapsulation and
629 controlled release properties. Int J Biol Macromol 116:1232-1239.

630 Lupetti A, Danesi R, Campa M, Del Tacca M, Kelly S (2002) Molecular basis of resistance to
631 azole antifungals. Trends Mol Med 8:76-81.

632 Marques CS, Carvalho SG, Bertoli LD, Villanova JCO, Pinheiro PF, dos Santos DCM, Yoshida
633 MI, de Freitas JCC, Cipriano DF, Bernardes PC (2019) β-Cyclodextrin inclusion
634 complexes with essential oils: Obtention, characterization, antimicrobial activity and
635 potential application for food preservative sachets. Food Res Int 119:499-509.

636 Pabast M, Shariatifar N, Beikzadeh S, Jahed G (2018) Effects of chitosan coatings incorporating
637 with free or nano-encapsulated Satureja plant essential oil on quality characteristics of
638 lamb meat. Food Control 91:185-192.

639 Perazzo FF, Carvalho JCT, Carvalho JE, Rehder VLG (2003) Central properties of the essential
640 oil and the crude ethanol extract from aerial parts of *Artemisia annua* L. Pharmacol
641 Res 48:497-502.

642 Pickova D, Ostry V, Malir J, Toman J, Malir F (2020) A Review on Mycotoxins and Microfungi
643 in Spices in the Light of the Last Five Years. Toxins 12:1-33.

644 Policegoudra RS, Goswami S, Aradhya SM, Chatterjee S, Datta S, Sivaswamy R, Chattopadhyay
645 P, Singh L (2012) Bioactive constituents of *Homalomena aromatica* essential oil and its
646 antifungal activity against dermatophytes and yeasts. J Mycol Méd 22: 83-87.

Potorti AG, Tropea A, Lo Turco V, Pellizzeri V, Belfita A, Dugo G, Di Bella G (2020) Mycotoxins in spices and culinary herbs from Italy and Tunisia. Nat Prod Res 34:167-171.

Prakash B, Kujur A, Yadav A, Kumar A, Singh PP, Dubey, N. K. (2018) Nanoencapsulation: An efficient technology to boost the antimicrobial potential of plant essential oils in food system. Food Control 89:1-11.

Rajkumar V, Gunasekaran C, Dharmaraj J, Chinnaraj P, Paul CA, Kanithachristy I (2020b) Structural characterization of chitosan nanoparticle loaded with *Piper nigrum* essential oil for biological efficacy against the stored grain pest control. Pestic Biochem Phys 166:1-9.

Rajkumar V, Gunasekaran C, Paul CA, & Dharmaraj J (2020a) Development of encapsulated peppermint essential oil in chitosan nanoparticles: characterization and biological efficacy against stored-grain pest control. Pestic Biochem Phys 170:1-9.

RASFF (2019) Rapid alert system for food and feed. Annual report-2019.https://ec.europa.eu/food/safety/rasff/index_en.htm

Rasooli I, Abyaneh MR (2004) Inhibitory effects of Thyme oils on growth and aflatoxin production by *Aspergillus parasiticus*. Food Control 15:479-483.

Ribeiro JC, Ribeiro WLC, Camurça-Vasconcelos ALF, Macedo ITF, Santos JML, Paula HCB, Filho JVA, Magalhaes RD, Bevilaqua CML (2014) Efficacy of free and nanoencapsulated *Eucalyptus citriodora* essential oils on sheep gastrointestinal nematodes and toxicity for mice. Vet Parasitol 204:243-248.

667 Ricci D, Fraternale D, Giamperi L, Bucchini A, Epifano F, Burini G, Curini M (2005) Chemical
668 composition, antimicrobial and antioxidant activity of the essential oil of *Teucrium*
669 *marum* (Lamiaceae). J Ethnopharmacol 98:195-200.

670 Roy SJ, Baruah PS, Lahkar L, Gurung L, Saikia D, Tanti B (2019) Phytochemical analysis and
671 antioxidant activities of *Homalomena aromatic* Schott. J Pharmacogn Phytochem *8*:1379-
672 1385.

673 Sathivel S, Liu Q, Huang J, Prinyawiwatkul W (2007) The influence of chitosan glazing on the
674 quality of skinless pink salmon (*Oncorhynchus gorbuscha*) fillets during frozen
675 storage. Journal Food Eng 83:366-373.

676 Schlosser I, Prange A (2018) Antifungal activity of selected natural preservatives against the
677 foodborne molds *Penicillium verrucosum* and *Aspergillus westerdijkiae*. FEMS
678 microbiology letters 365: fny125.

679 Sheijooni-Fumani N, Hassan J, Yousefi SR (2011) Determination of aflatoxin B_1 in cereals by
680 homogeneous liquid–liquid extraction coupled to high performance liquid
681 chromatography-fluorescence detection. J Sep Sci 34:1333-1337.

682 Singh A, Chaudhari AK, Das S, Singh VK, Dwivedy AK, Shivalingam RK, Dubey NK (2020b)
683 Assessment of preservative potential of *Bunium persicum* (Boiss) essential oil against
684 fungal and aflatoxin contamination of stored masticatories and improvement in efficacy
685 through encapsulation into chitosan nanomatrix. Environ Sci Pollut Res 27:27635-27650.

686 Singh N, Rao AS, Nandal A, Kumar S, Yadav SS, Ganaie SA, Narasimhan B (2020a)
687 Phytochemical and pharmacological review of *Cinnamomum verum* J. Presl-a versatile
688 spice used in food and nutrition. Food Chem 338:1-24.

689 Siva S, Li C, Cui H, Meenatchi V, Lin L (2020) Encapsulation of essential oil components with
690 methyl-β-cyclodextrin using ultrasonication: Solubility, characterization, DPPH and
691 antibacterial assay. Ultrason Sonochem 64*:*1-12.

692 Su H, Huang C, Liu Y, Kong S, Wang J, Huang H, Zhang B (2020) Preparation and
693 characterization of Cinnamomum essential oil–chitosan nanocomposites: Physical,
694 Structural, and Antioxidant Activities. Processes 8:1-13.

695 Thanushree MP, Sailendri D, Yoha KS, Moses JA, Anandharamakrishnan C (2019) Mycotoxin
696 contamination in food: An exposition on spices. Trends Food Sci Technol 93:69-80.

697 Tian J, Huang B, Luo X, Zeng H, Ban X, He J, Wang Y (2012) The control of *Aspergillus flavus*
698 with *Cinnamomum jensenianum* Hand.-Mazz essential oil and its potential use as a food
699 preservative. Food Chem 130:520-527.

700 Tsikas D (2017) Assessment of lipid peroxidation by measuring malondialdehyde (MDA) and
701 relatives in biological samples: Analytical and biological challenges. Anal Biochem
702 524:13-30.

703 Upadhyay N, Singh VK, Dwivedy AK, Das S, Chaudhari AK, Dubey NK (2018) *Cistus*
704 *ladanifer* L. essential oil as a plant based preservative against molds infesting oil seeds,
705 aflatoxin B_1 secretion, oxidative deterioration and methylglyoxal biosynthesis. LWT-
706 Food Sci Technol 92:395-403.

Wu L, Liu M (2008) Preparation and properties of chitosan-coated NPK compound fertilizer with controlled-release and water-retention. Carbohydr Polym 72:240-247.

Yadav SK, Singla-Pareek SL, Reddy MK, Sopory SK (2005) Transgenic tobacco plants overexpressing glyoxalase enzymes resist an increase in methylglyoxal and maintain higher reduced glutathione levels under salinity stress. Federation of European Biochemical Societies (FEBS) Letters 579:6265-6271.

Yang Z, Wang H, Ying G, Yang M, Nian Y, Liu J, Kong W (2017) Relationship of mycotoxins accumulation and bioactive components variation in ginger after fungal inoculation. Front Pharmacol 8:331.

Zabka M, Pavela R, Slezakova L (2009) Antifungal effect of *Pimenta dioica* essential oil against dangerous pathogenic and toxinogenic fungi. Ind Crops Prod 30:250-253.

Zhu JJ, Zeng XP, Berkebile D, Du HJ, Tong Y, Qian K (2009) Efficacy and safety of catnip (*Nepeta cataria*) as a novel filth fly repellent. Med Vet Entomol 23:209-216.

Figures

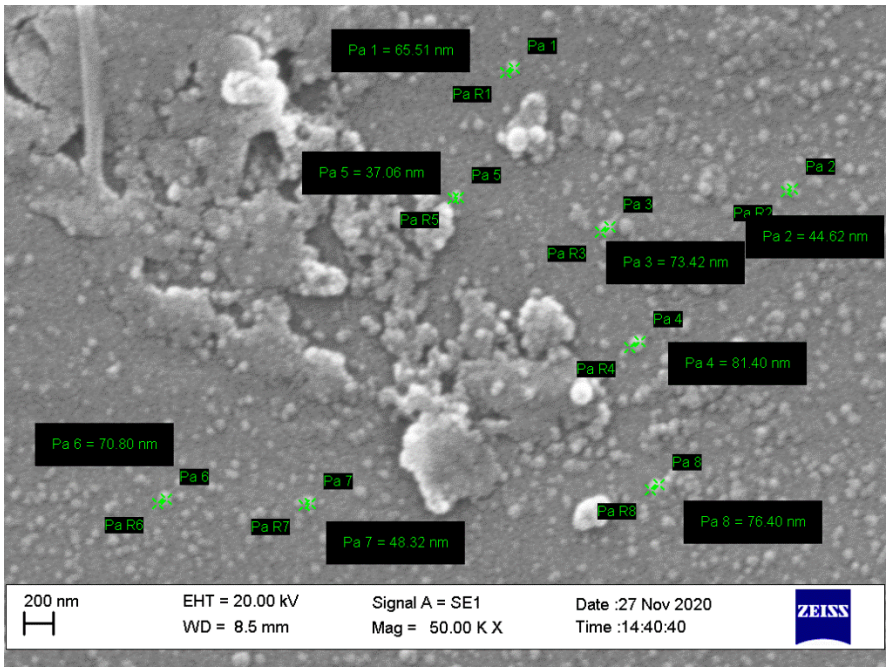
Pa 1 = 65.51 nm
Pa 1
Pa R1
Pa 5 = 37.06 nm
Pa 5
Pa 2
Pa 3
Pa R5
Pa 2 = 44.62 nm
Pa R3
Pa 3 = 73.42 nm
Pa 4
Pa 4 = 81.40 nm
Pa R4
Pa 6 = 70.80 nm
Pa 8
Pa 6
Pa 7
Pa R6
Pa R7
Pa R8
Pa 8 = 76.40 nm
Pa 7 = 48.32 nm
200 nm
EHT = 20.00 kV
WD = 8.5 mm
Signal A = SE1
Mag = 50.00 K X
Date :27 Nov 2020
Time :14:40:40
ZEISS

(A)

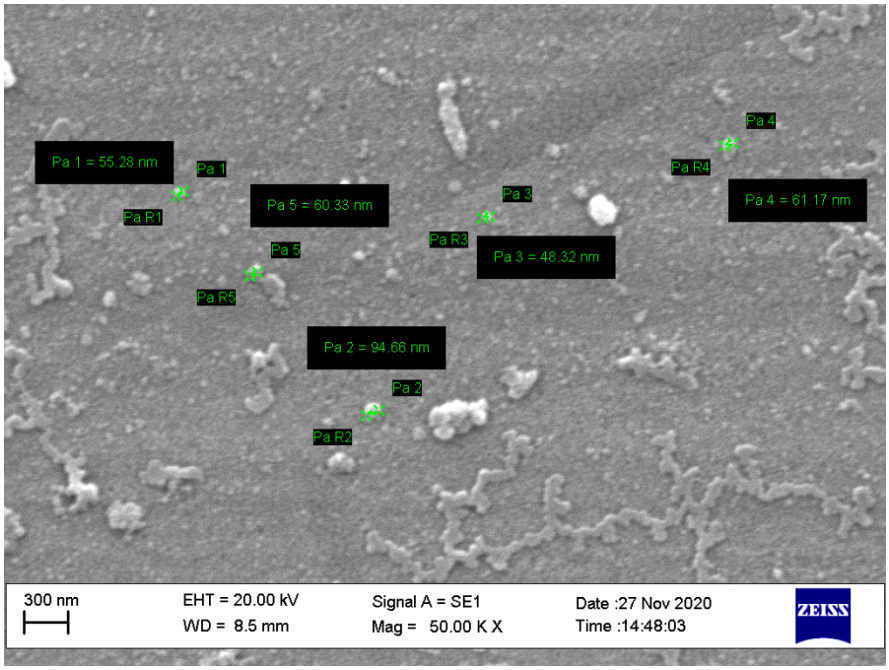

739

740 (B)

741 **Fig. 1** SEM image of (A) CS Ne and (B) CS-HAEO-Ne

742

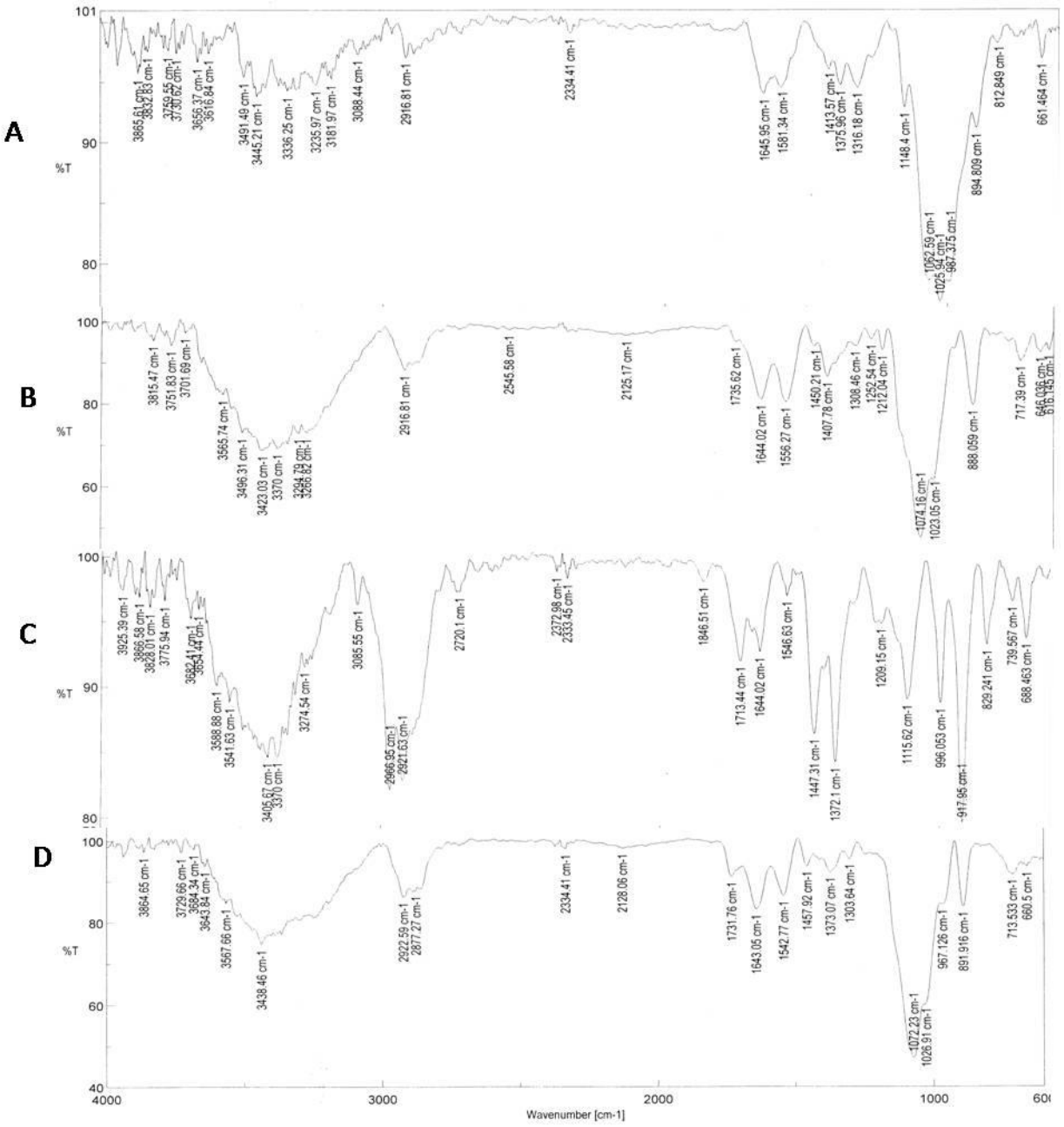

743

744 **Fig. 2** FTIR spectra of (A) CS, (B) CS Ne, (C) EO and (D) CS-HAEO-Ne

745

746

747

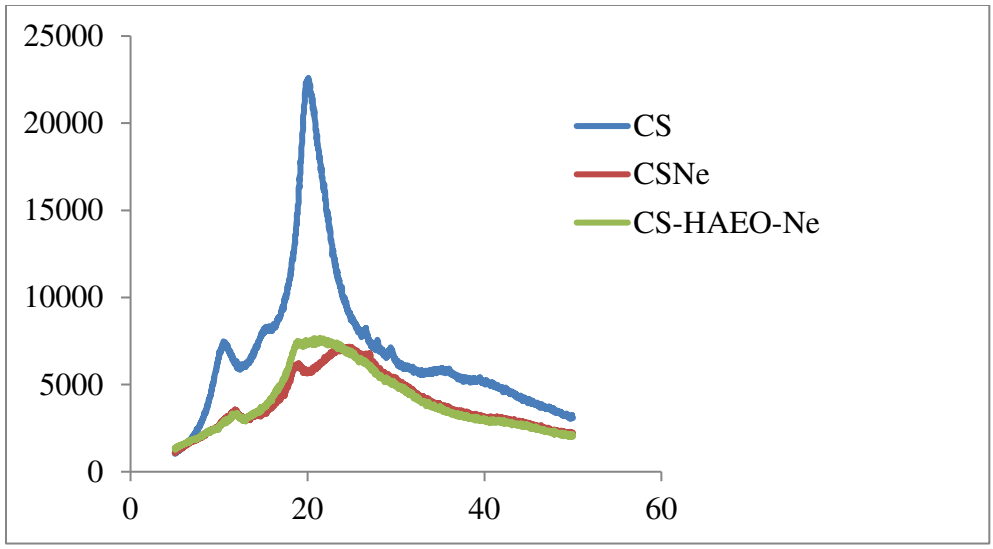

748

749 **Fig. 3** XRD spectra of CS, CS Ne and CS-HAEO-Ne

750

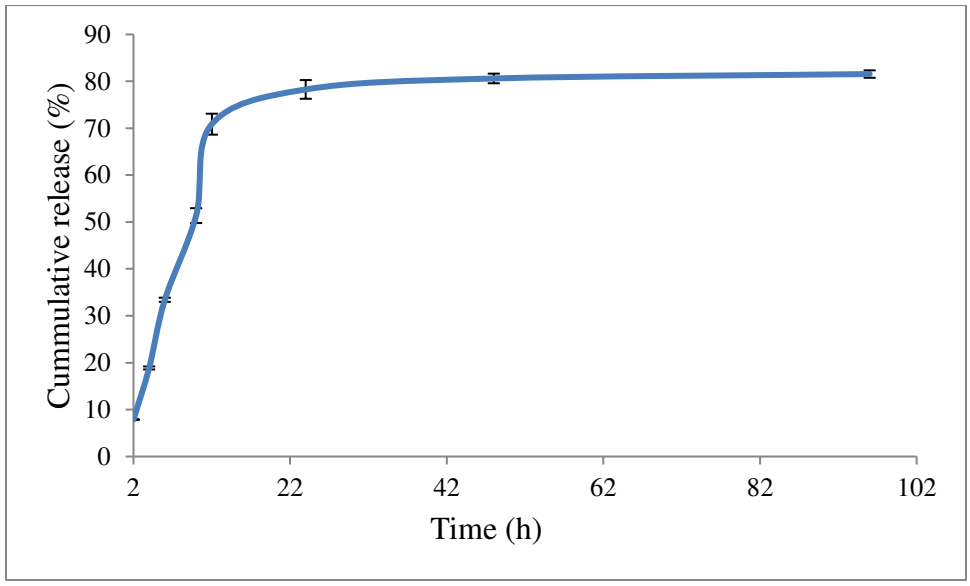

751

752 **Fig. 4** *In vitro* release profile of CS-HAEO-Ne

753

754

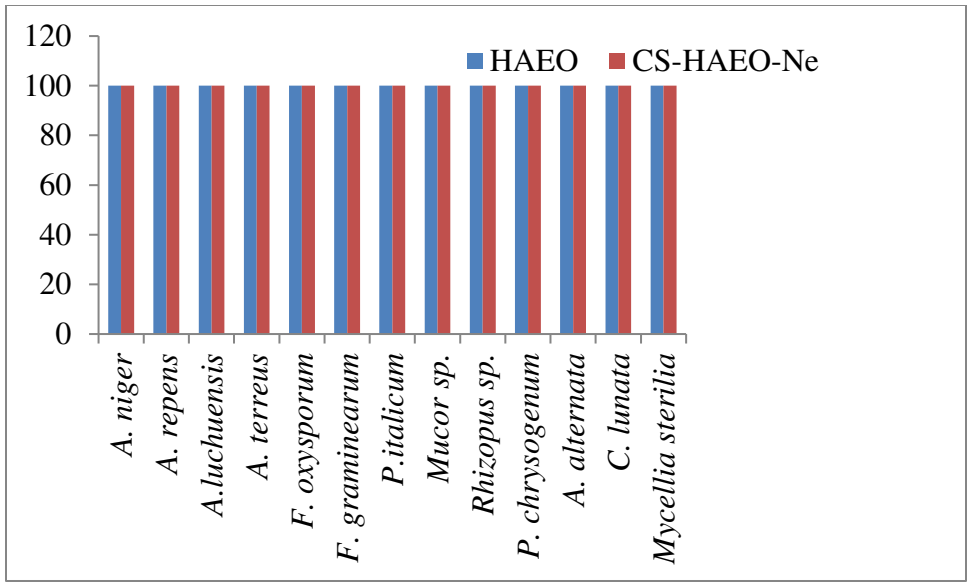

Fig. 5 Fungitoxic spectrum of HAEO and CS-HAEO-Ne at their respective MIC concentration

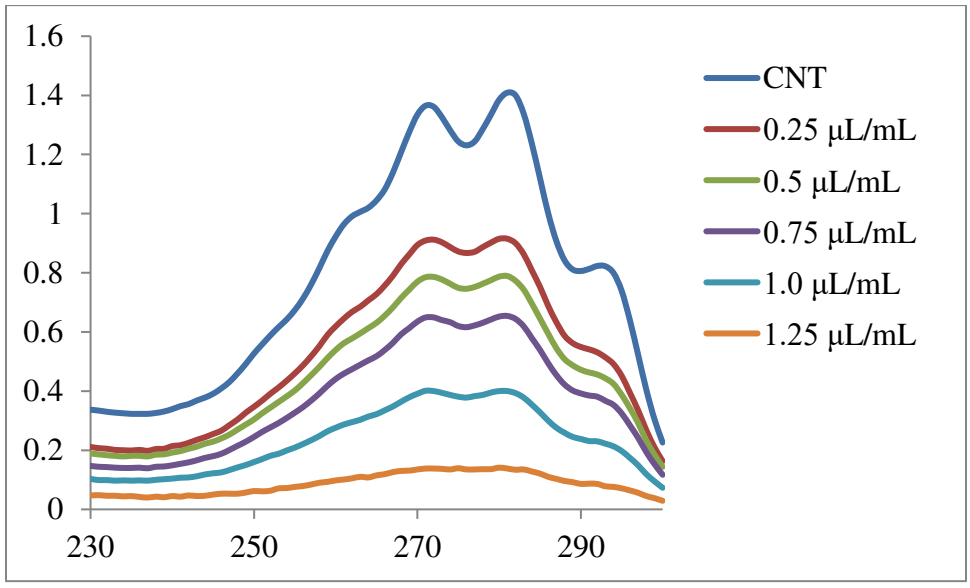

(A)

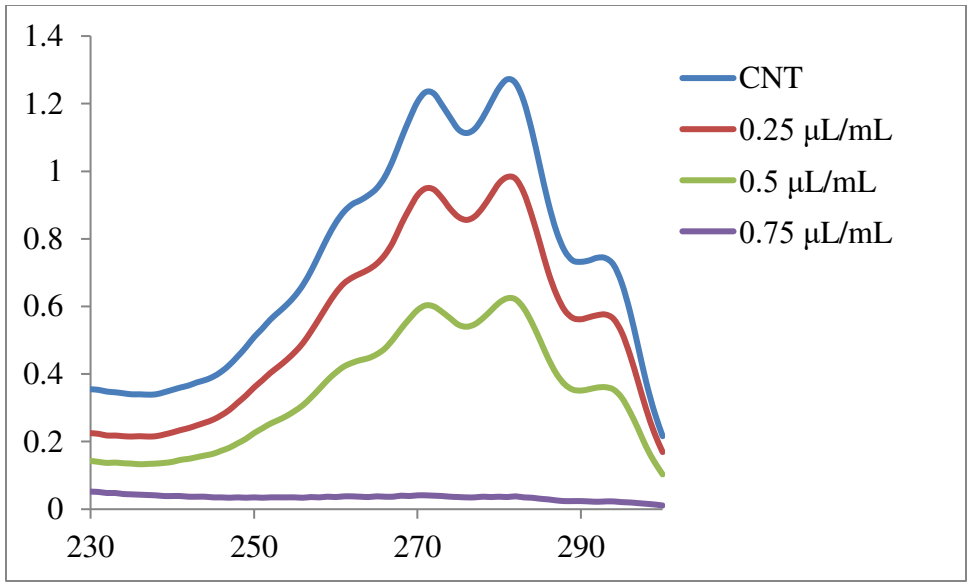

(B)

Fig. 6 Ergosterol inhibition at different concentration of (A) HAEO and (B) CS-HAEO-Ne

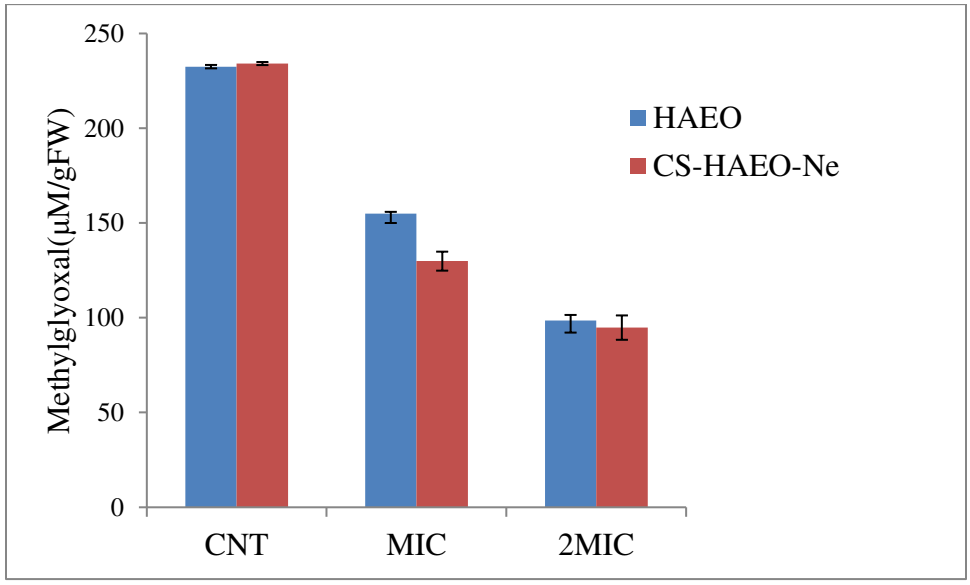

Fig. 7 Effect of (A) HAEO and (B) CS-HAEO-Ne on methylglyoxal of AF-LHP NS 7

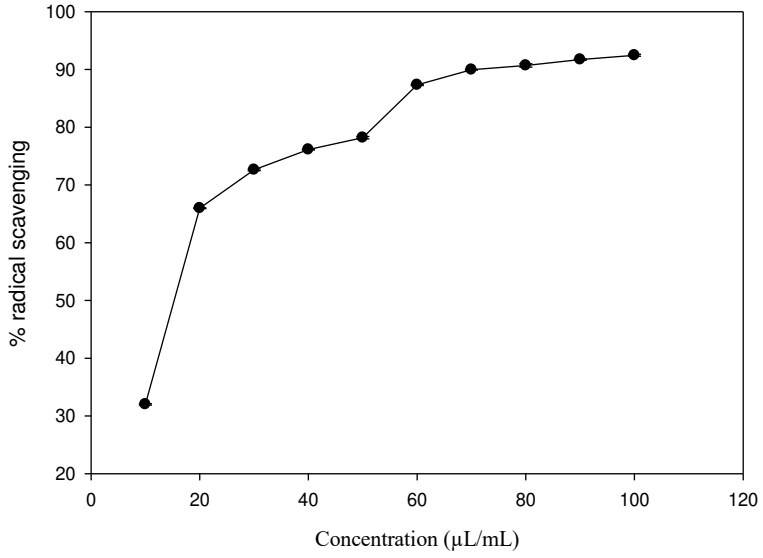

768

769 (A)

770

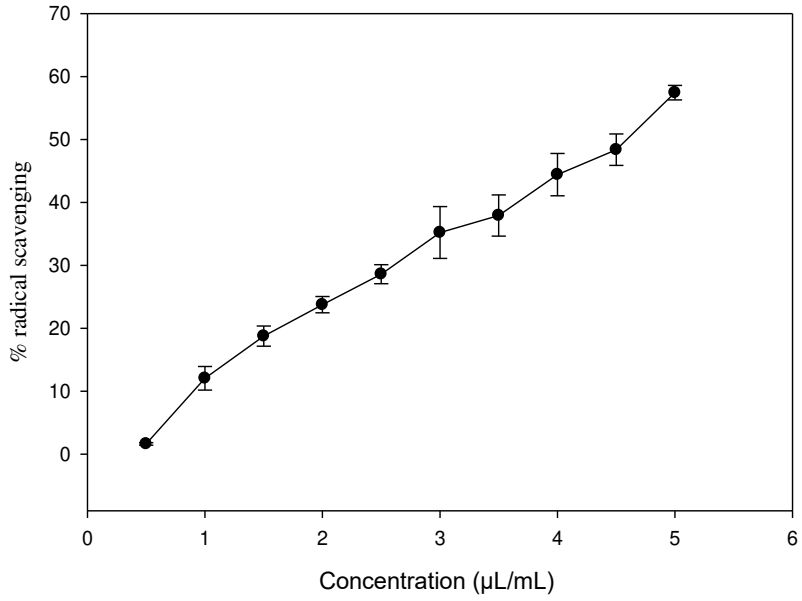

771

772 (B)

773 **Fig. 8** DPPH free radical scavenging activity of (A) HAEO and (B) CS-HAEO-Ne

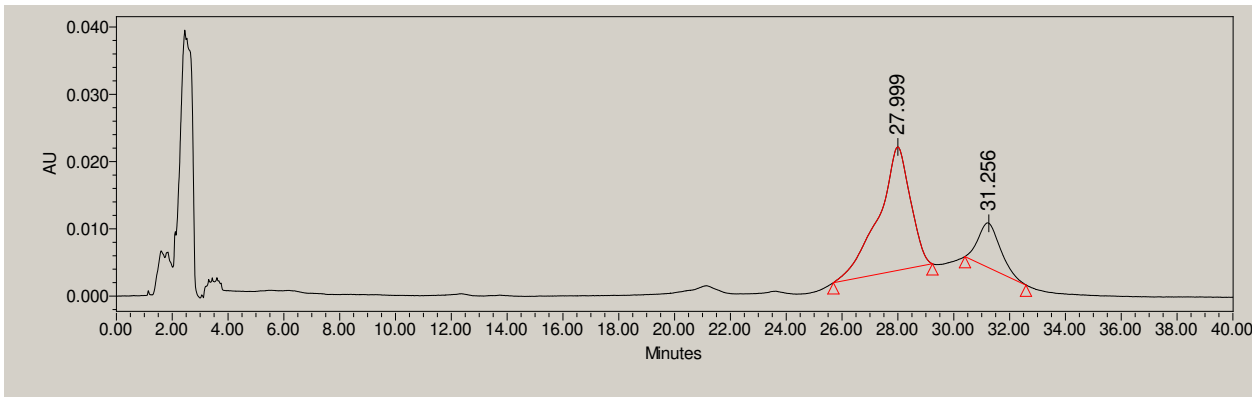

774

775 (A)

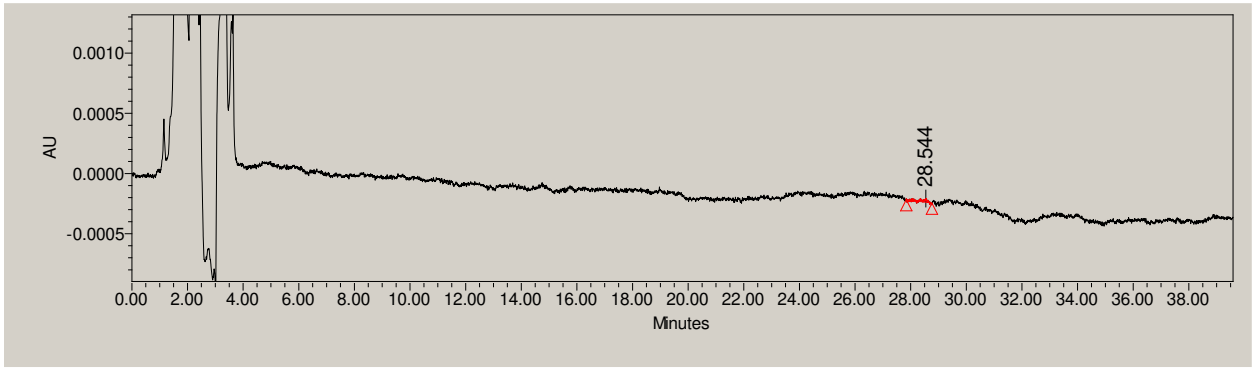

776

777 (B)

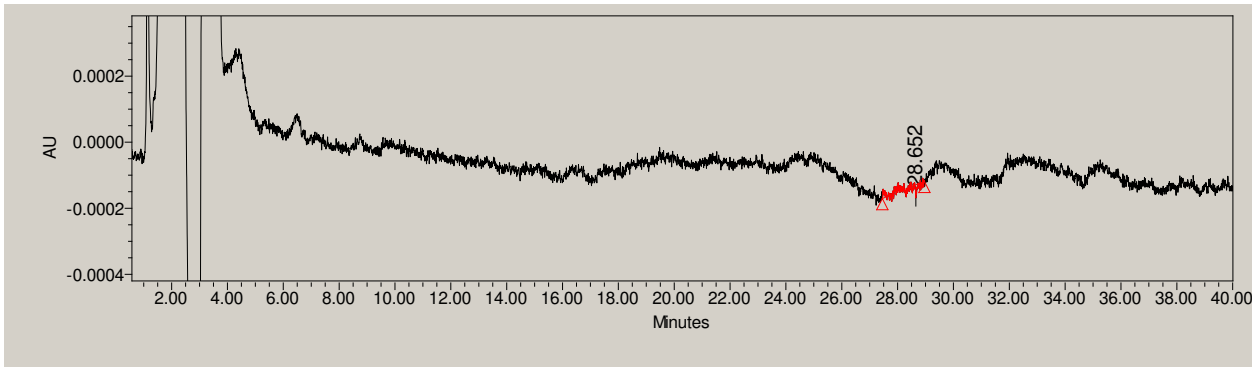

778

779 (C)

780 **Fig. 9** *In vivo* antiaflatoxigenic efficacy of HAEO and CS-HAEO-Ne; (A) CNT, (B) HAEO and
781 (C) CS-HAEO-Ne

782

783

784 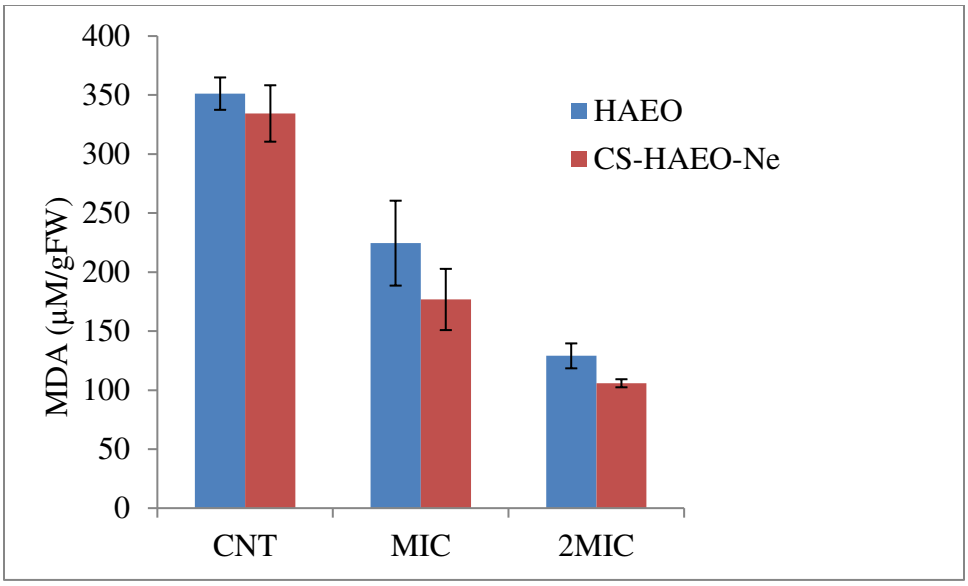

785 **Fig. 10** Effect of HAEO and CS-HAEO-Ne fumigation on lipid peroxidation of stored black
786 cumin (*Nigella sativa*) seeds

787

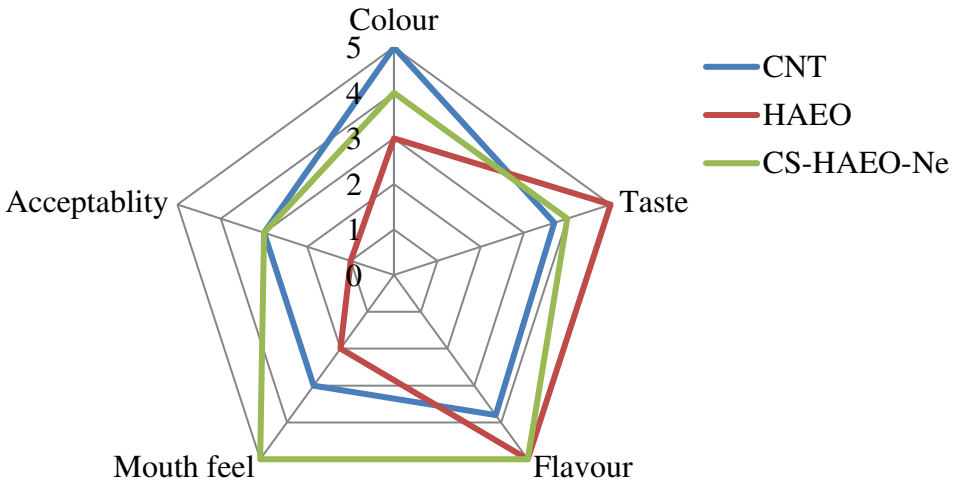

788

789 **Fig. 11** Sensorial profile of HAEO and CS-HAEO-Ne fumigated black cumin (*Nigella sativa*)
790 seed

791

792

793

Table 1 Chemical Profile of *Homalomena aromatica* essential oil (HAEO)

S.NO.	Bioactive Components	Retention time	Percentage
1	Terpinolene	4.91	0.23
2	β-pinene	5.25	0.28
3	α-pinene	5.75	3.16
4	α-terpinene	5.89	0.45
5	o-cymene	6.13	1.04
6	D-limonene	6.21	1.21
7	β-ocimene	6.72	0.09
8	γ-terpinene	7.05	1.1
9	Linalool oxide	7.57	0.33
12	**Linalool**	8.44	68.51
13	Hotrienol	8.62	0.2
14	**Terpinen-4-ol**	11.06	8.26
15	m-cymen-8-ol	11.48	0.28
16	Terpineol	11.61	2.24
17	cis-geraniol	13.14	0.35
18	Geraniol	14.16	0.81
19	Espatulenol	26.49	0.57
20	Globulol	27.35	0.14
21	Tau-cadinol acetate	28.76	0.35
22	α-cadinol	28.8	0.64
23	Caryophyllene oxide	30.46	1.47
		Total	91.71

Note: Compounds in bold are major components

Table 2 % nanoencapsulation efficiency and % loading capacity of HAEO inside chitosan polymeric matrix

Chitosan: HAEO (w/v)	NEE %	LC %
1:0.0	0.00 ± 0.00^{a}	0.00 ± 0.00^{a}
1:0.2	22.01 ± 0.25^{b}	0.15 ± 0.00^{b}
1:0.4	24.82 ± 0.37^{c}	0.35 ± 0.01^{c}
1:0.6	55.68 ± 0.25^{d}	1.16 ± 0.01^{d}
1:0.8	**83.42 ± 0.38^{e}**	**2.32 ± 0.01^{e}**
1:1	60.07 ± 0.05^{f}	2.08 ± 0.00^{f}

NEE= nanoencapsulation efficiency, LC= Loading capacity
Values are mean (n=3) ± standard error
Significance difference between the means ($p < 0.05$, ANOVA test)

Table 3 Effect of HAEO and CS-HAEO-Ne on mycelial dry weight (MDW) and AFB_1 production by AF-LHP-NS 7

Concentration (µL/mL)	HAEO			CS-HAEO-Ne		
	MDW (g)	AFB_1 (µg/mL)	% inhibition	MDW (g)	AFB_1 (µg/mL)	% inhibition
CNT	0.69±0.03[a]	3.94±0.05[a]	0	0.67±0.01[a]	3.76±0.05[a]	0
0.25	0.63±0.01[a]	3.76±0.07[b]	4.74	0.55±0.00[b]	3.39±0.05[b]	9.92
0.50	0.53±0.00[a]	2.74±0.04[c]	30.47	0.38±0.01[c]	2.42±0.07[c]	35.54
0.75	0.47±0.00[b]	2.38±0.06[d]	39.78	0.29±0.01[d]	1.53±0.05[d]	59.29
1.0**	0.22±0.07[c]	0.34±0.02[e]	92.57	0.13±0.01[e]	0.00±0.00[e]	100
1.25*	0.00±0.00[cd]	0.00±0.00[f]	100	0.00±0.00[f]	-	-
1.5	0.00±0.00[d]	0.00±0.00	-	-	-	-
1.75	0.00±0.00[e]	0.00±0.00	-	-	-	-

AFB_1 = aflatoxin B_1

Values are mean (n = 3) ± standard error

Significance difference between the means ($p<0.05$, ANOVA test)

CNT = Control

Table 4 Effect of HAEO and CS-HAEO-Ne on vital cellular constituent's release of AF-LHP-NS 7

Conc. (µL/mL)	Leakage of vital cellular constituents									
	Ca^{+2} (mg/L)		Mg^{+2} (mg/L)		K^{+} (mg/L)		260 nm absorbing material		280 nm absorbing material	
	HAEO	**CS-HAEO-Ne**	**HAEO**	**CS-HAEO-Ne**	**HAEO**	**CS-HAEO-Ne**	**HAEO**	**CS-HAEO-Ne**	**HAEO**	**CS-HAEO-Ne**
CNT	6.57±0.73^{a}	2.83±0.95^{a}	4.70±2.14^{a}	3.98±0.46^{a}	3.48±0.67^{a}	11.90±1.75^{a}	0.69±0.21^{a}	0.10±0.00^{a}	0.37±0.28^{a}	0.12±0.01^{a}
0.25	9.35±0.85^{a}	8.92±0.62^{b}	6.48±1.32^{ab}	8.20±1.41^{bc}	30.22±2.05^{b}	42.10±2.39^{ab}	0.087±0.00^{a}	0.13±0.00^{a}	0.10±0.00^{a}	0.16±0.00^{a}
0.50	6.55±2.59^{ab}	10.72±1.35^{bc}	7.85±0.88^{abc}	8.55±1.39^{bc}	40.1±4.95^{bc}	81.50±11.57^{abc}	0.15±0.00^{a}	0.34±0.01^{b}	0.13±0.00^{a}	0.32±0.01^{b}
0.75	10.50±0.90^{ab}	12.43±1.01^{bc}	9.18±0.43^{abc}	9.40±1.20^{c}	51.48±5.69^{bcd}	91±11.03^{bc}	0.16±0.00^{ab}	0.46±0.01^{c}	0.23±0.01^{b}	0.57±0.01^{c}
1.0	12.13±1.42^{ab}	14.15±0.635^{c}	10.42±0.76^{abcd}	10.15±0.78^{c}	56.38±5.21^{cd}	107±15.17^{bc}	0.25±0.03^{ab}	0.54±0.01^{d}	0.34±0.01^{c}	0.77±0.01^{d}
1.25*	13.38±1.09^{ab}	18.72±0.32^{d}	12.52±1.21^{bcd}	13.05±0.73^{c}	59.17±4.23^{cd}	118±22.31^{c}	0.31±0.01^{ab}	0.65±0.01^{e}	0.37±0.01^{c}	0.87±0.03^{d}
1.5	16.07±2.14^{ab}	-	13.10±1.49^{cd}	-	67.33±6.50^{de}	-	0.32±0.02^{ab}	-	0.47±0.01^{d}	-
1.75**	20.35±4.41^{b}	-	15.67±1.45^{d}	-	72.33±8.64^{de}	-	0.54±0.01^{bc}	-	0.58±0.00^{e}	-
2MIC	37.20±5.59^{c}	38.08±1.77^{e}	23.78±1.48^{e}	25.92±1.44^{d}	85.97±5.07^{e}	154±9.83^{d}	0.68±0.02^{c}	0.94±0.04^{f}	0.64±0.02^{f}	1.36±0.09^{e}

* =Minimum inhibitory concentration for CS-HAEO-Ne, ** =Minimum inhibitory concentration for HAEO, - = not measured

Values are mean(n=3) ± standard error

Significance difference between the means ($p < 0.05$, ANOVA test)

819 **Table 5** Effect of HAEO and CS-HAEO-Ne on *in situ* mineral content of black cumin seeds

Samples	Mineral contents (mg/L)					
	Potassium (K)	**Calcium (Ca)**	**Magnesium (Mg)**	**Iron (Fe)**	**Zinc (Zn)**	**Manganese (Mn)**
HAEO CNT	55.77±11.03^{a}	63.17±5.70^{a}	4.55±0.52^{a}	1.87±0.26^{a}	1.55±0.13^{a}	0.88±0.61^{a}
HAEO MIC	79.33±7.37^{ab}	180.17±9.94^{a}	20.18±0.77^{a}	12.88±1.08^{a}	6.28±0.28^{a}	2.1±1.15^{a}
CS-HAEO-Ne CNT	40.33±0.81^{bc}	77±1.76^{b}	5±0.36^{b}	2.35±0.92^{b}	2.9±0.65^{b}	0.45±0.17^{b}
CS-HAEO-Ne MIC	95±3.75^{c}	194.5±13.60^{b}	22.8±0.82^{c}	14.56±0.57^{b}	5.82±0.16^{b}	2.2±1.21^{b}

820 Values are mean (n=3) ± standard error

821 Significance difference between the means ($p < 0.05$, ANOVA test)

Figures

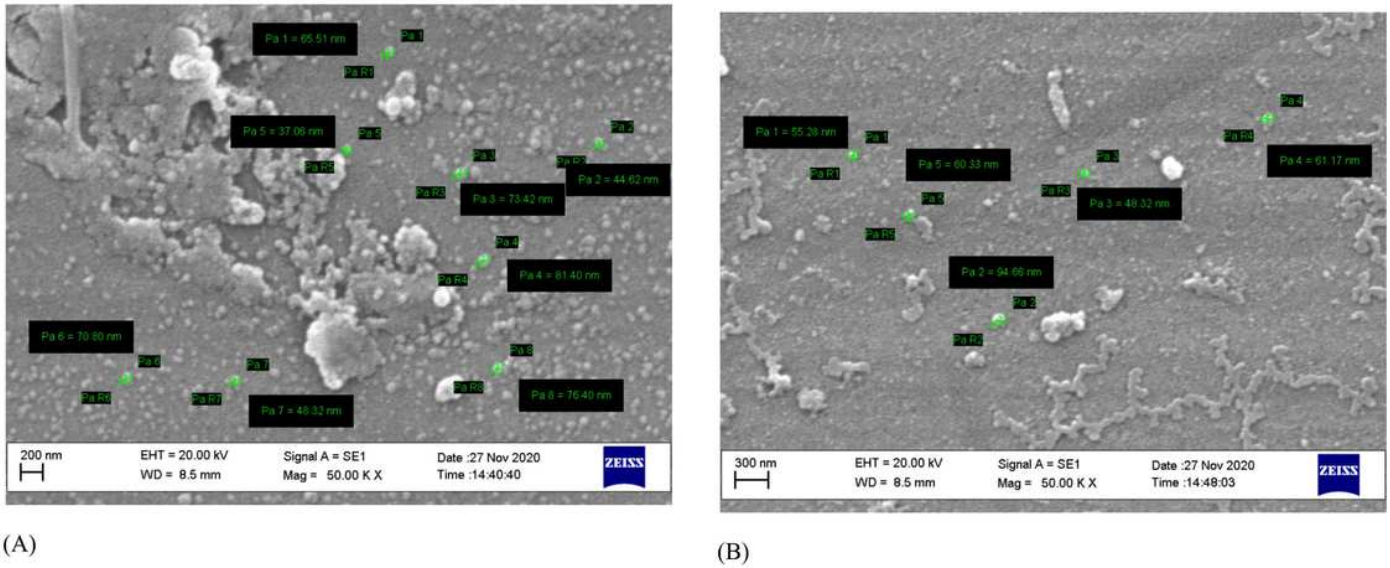

Figure 1

SEM image of (A) CS Ne and (B) CS-HAEO-Ne

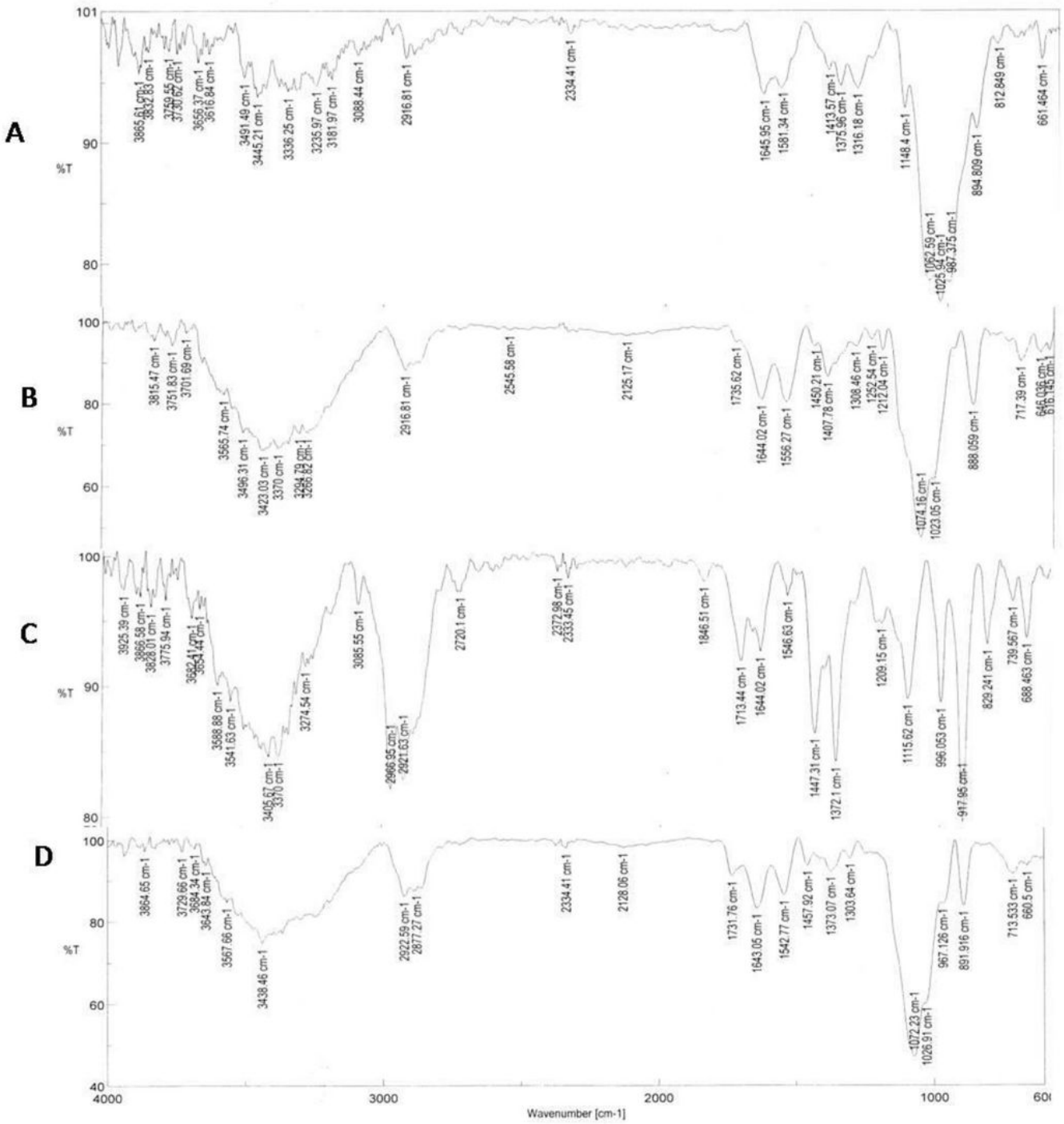

Figure 2

FTIR spectra of (A) CS, (B) CS Ne, (C) EO and (D) CS-HAEO-Ne

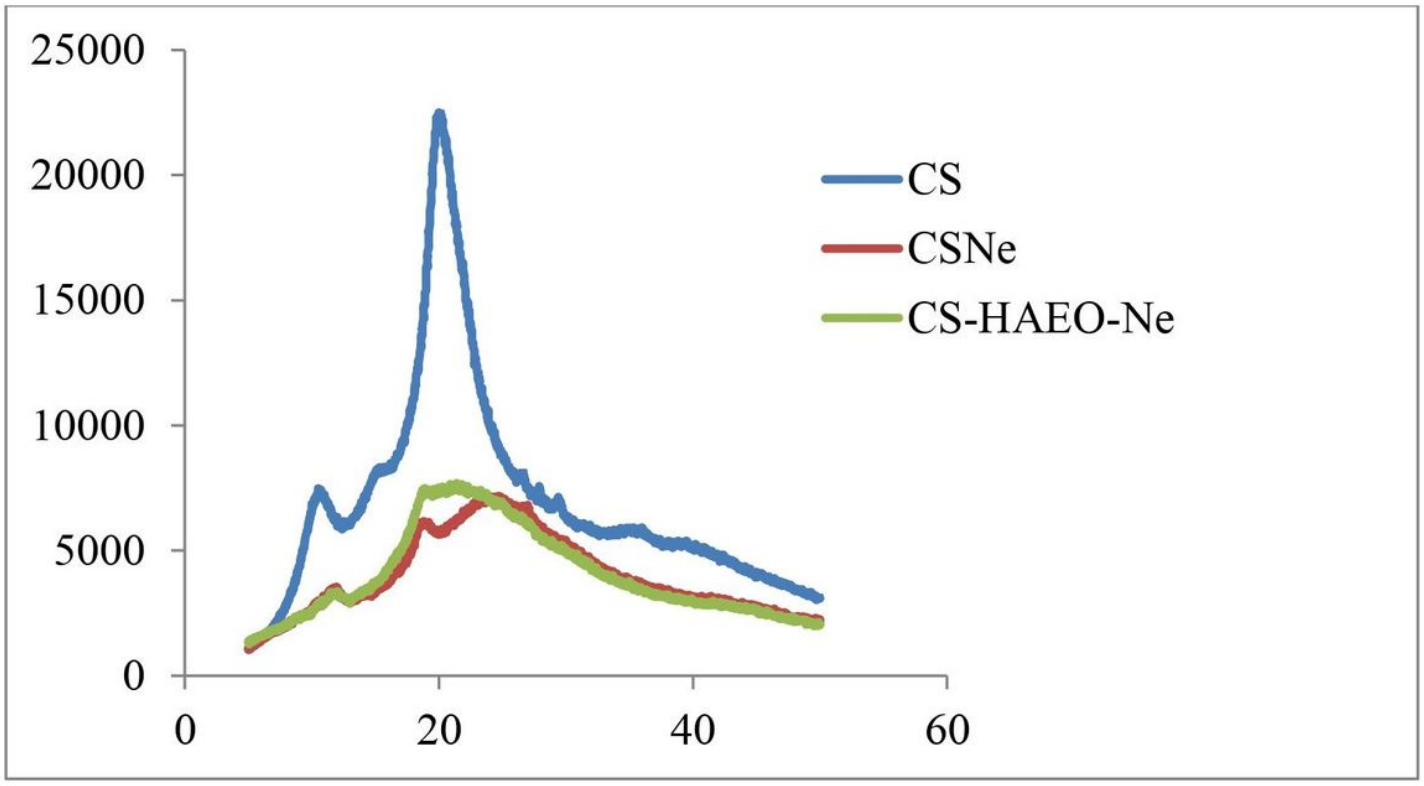

Figure 3

XRD spectra of CS, CS Ne and CS-HAEO-Ne

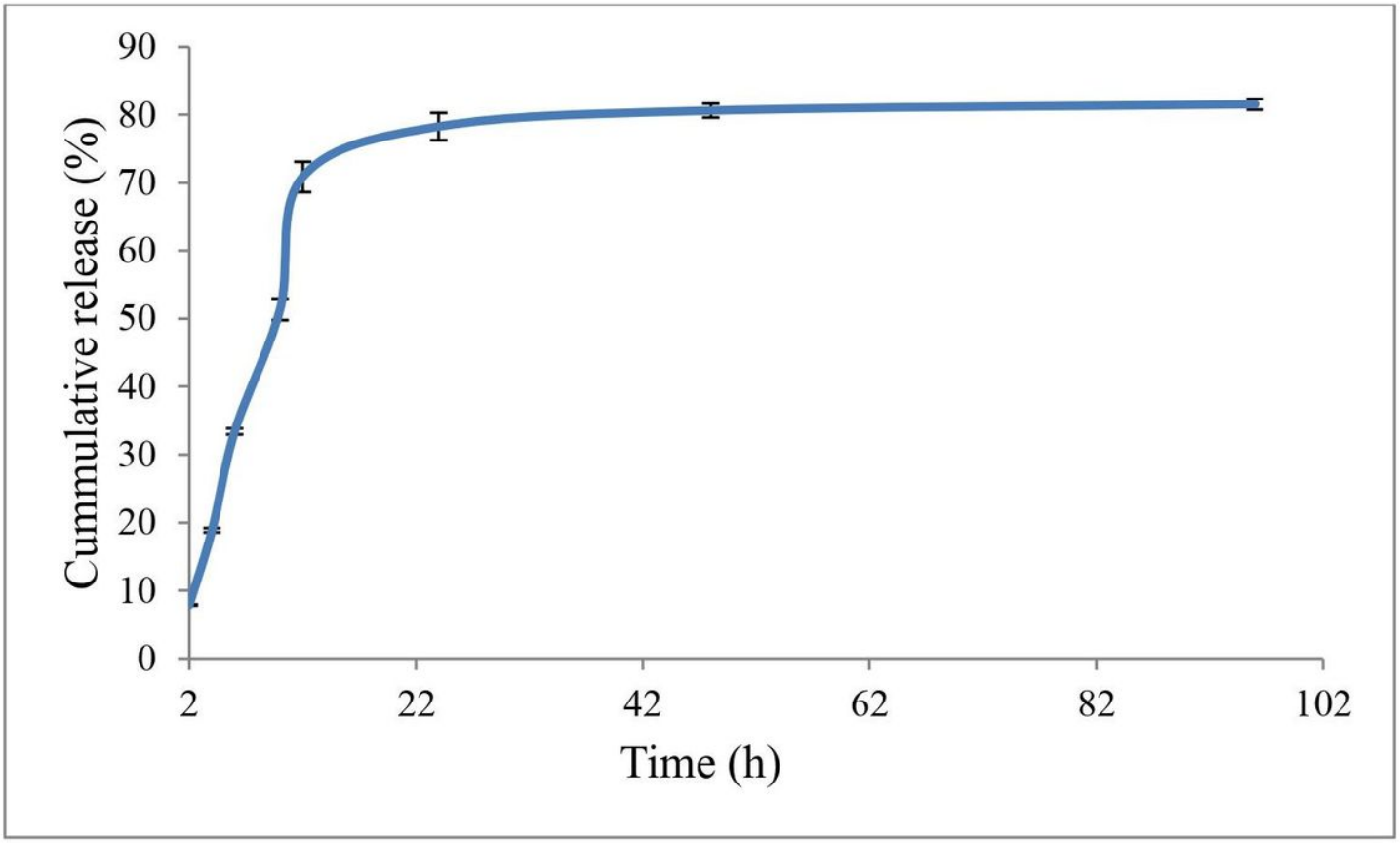

Figure 4

In vitro release profile of CS-HAEO-Ne

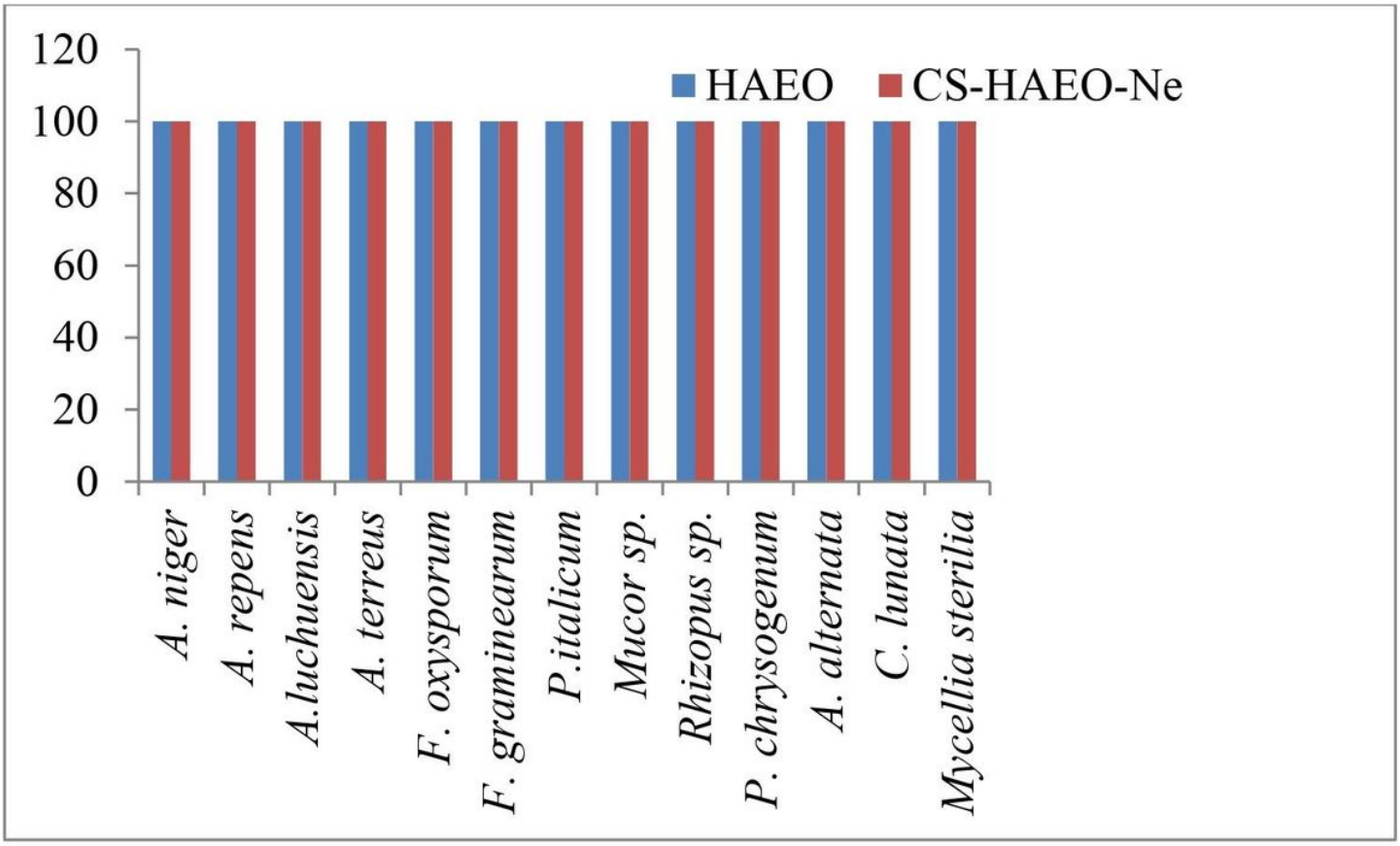

Figure 5

Fungitoxic spectrum of HAEO and CS-HAEO-Ne at their respective MIC concentration

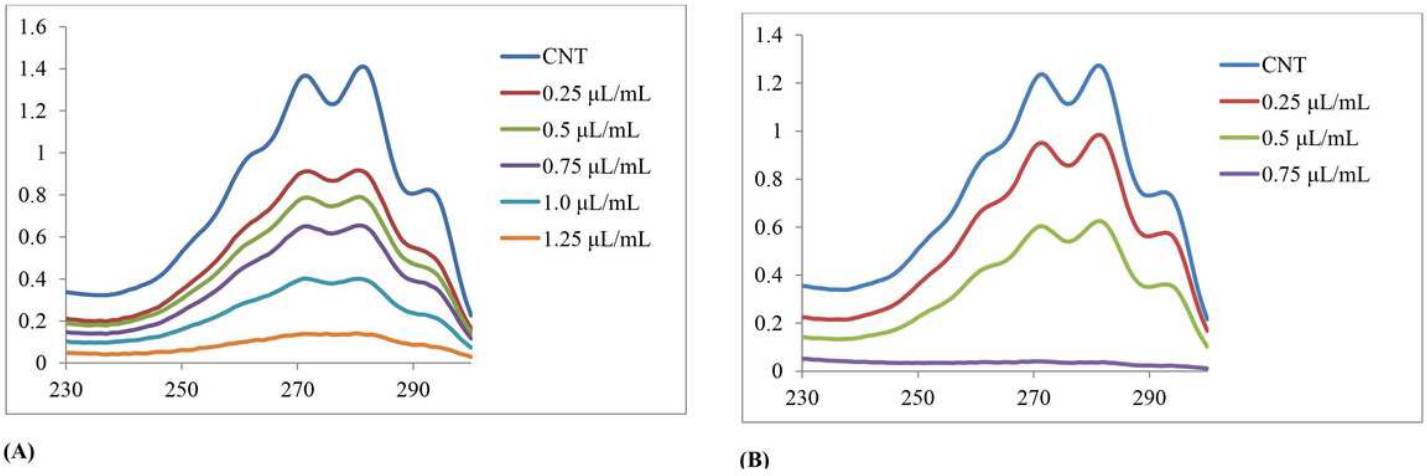

Figure 6

Ergosterol inhibition at different concentration of (A) HAEO and (B) CS-HAEO-Ne

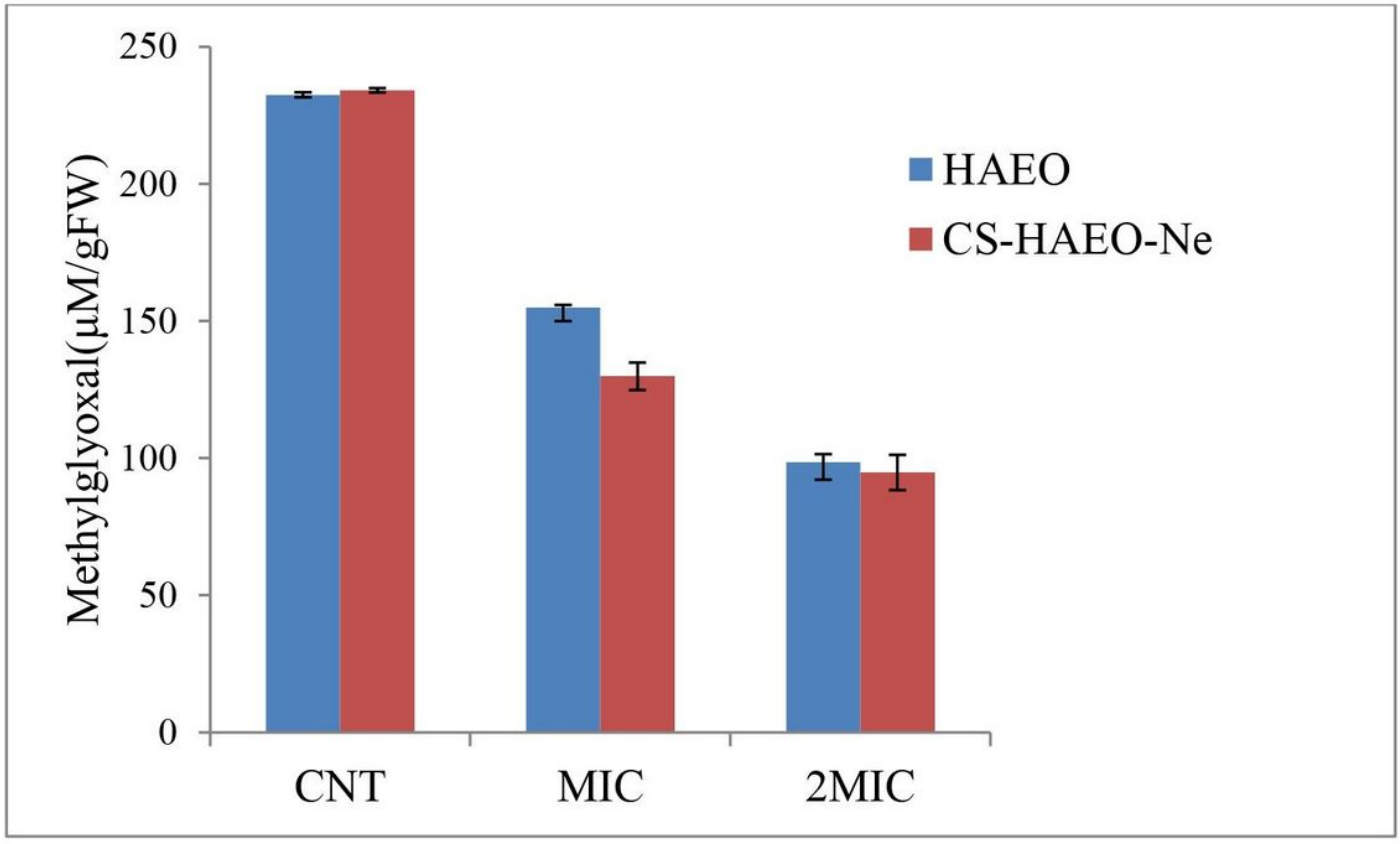

Figure 7

Effect of (A) HAEO and (B) CS-HAEO-Ne on methylglyoxal of AF-LHP NS 7

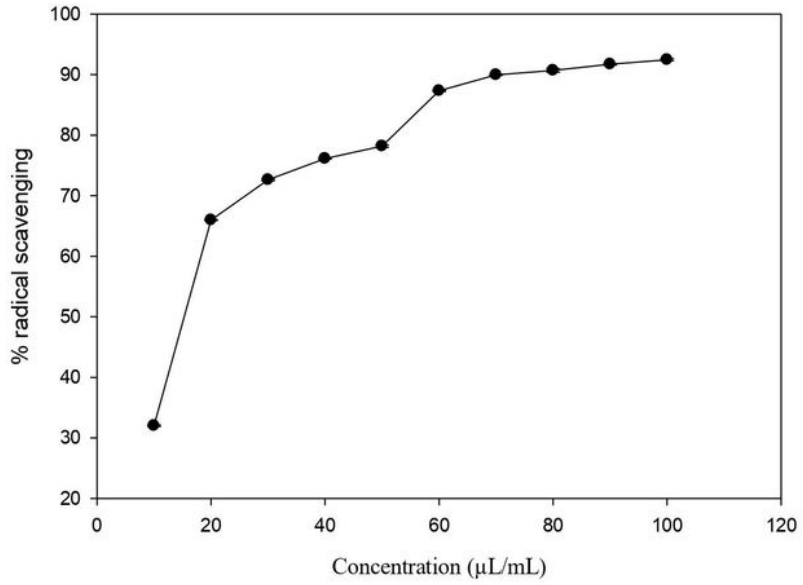

(A)

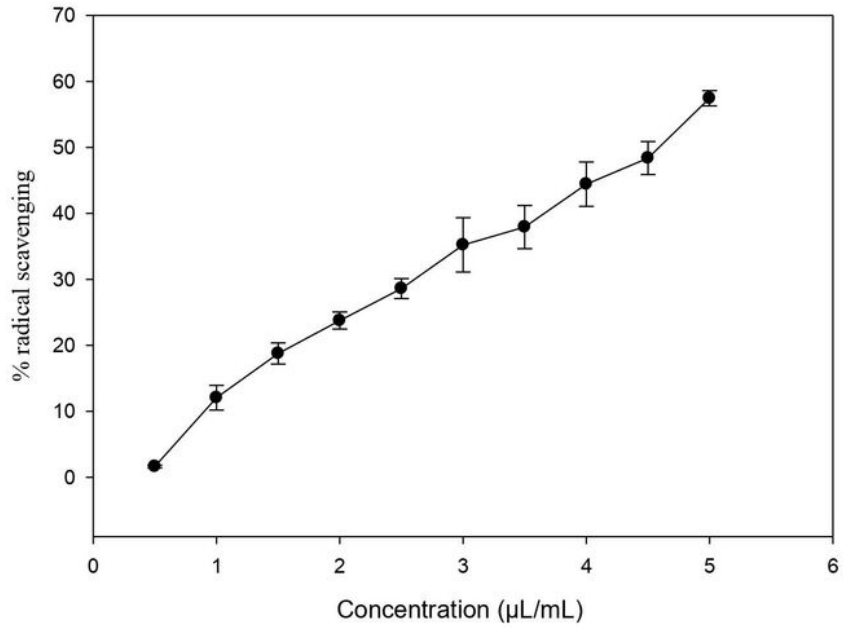

(B)

Figure 8

DPPH free radical scavenging activity of (A) HAEO and (B) CS-HAEO-Ne

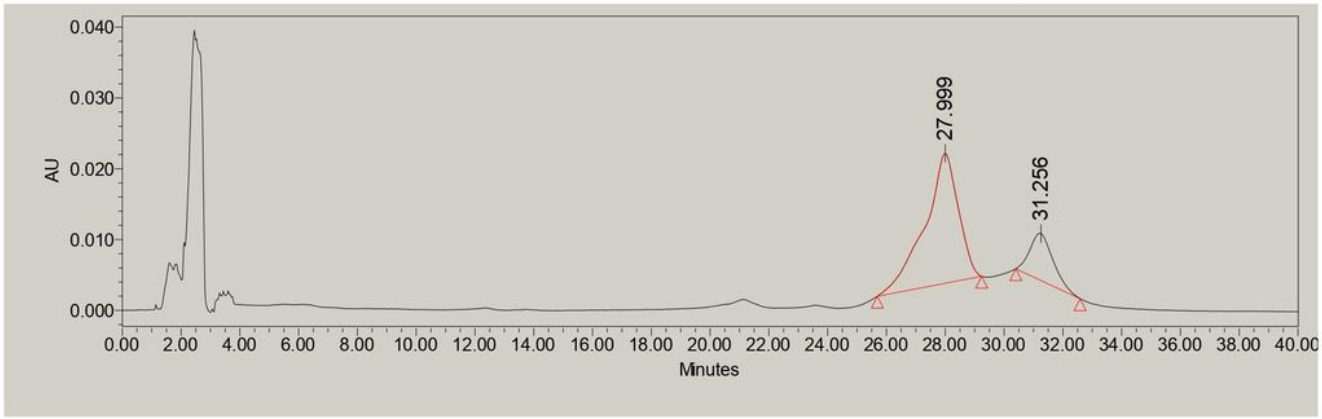

(A)

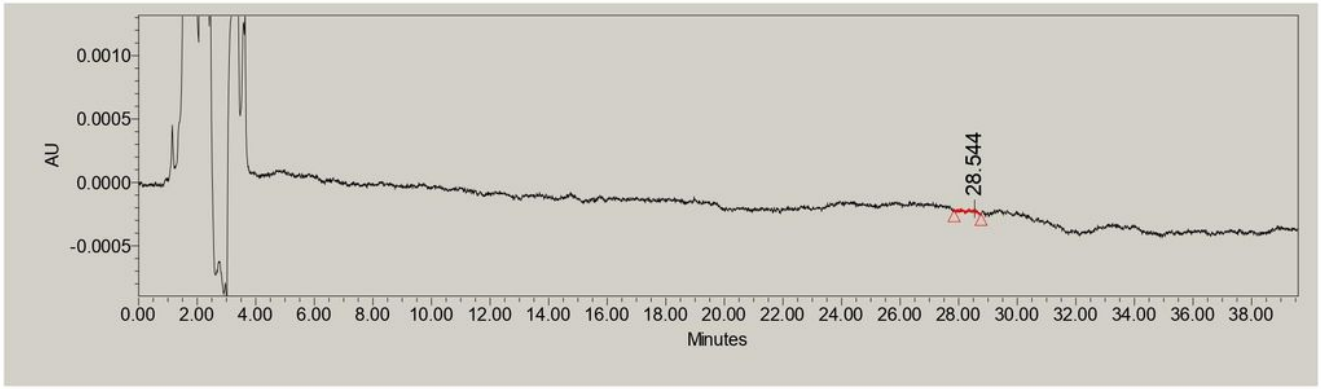

(B)

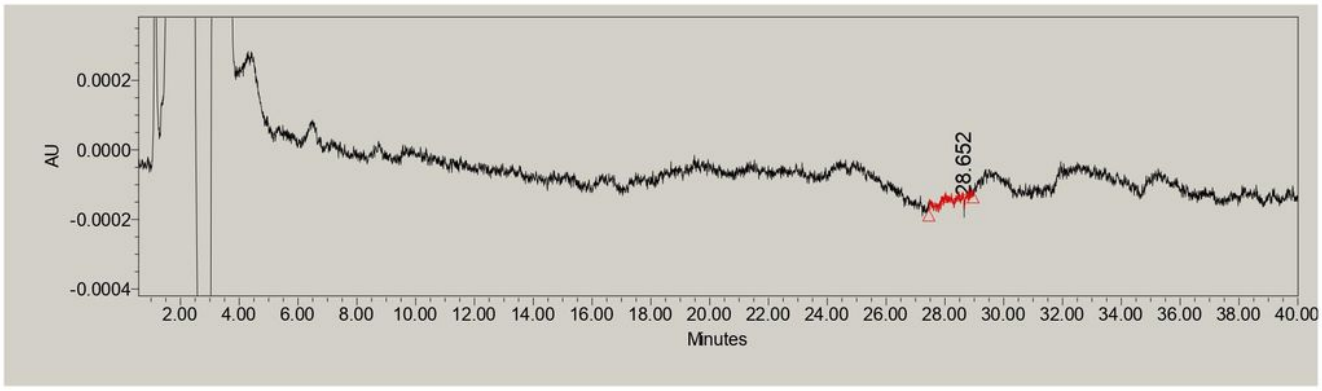

(C)

Figure 9

In vivo antiaflatoxigenic efficacy of HAEO and CS-HAEO-Ne; (A) CNT, (B) HAEO and (C) CS-HAEO-Ne

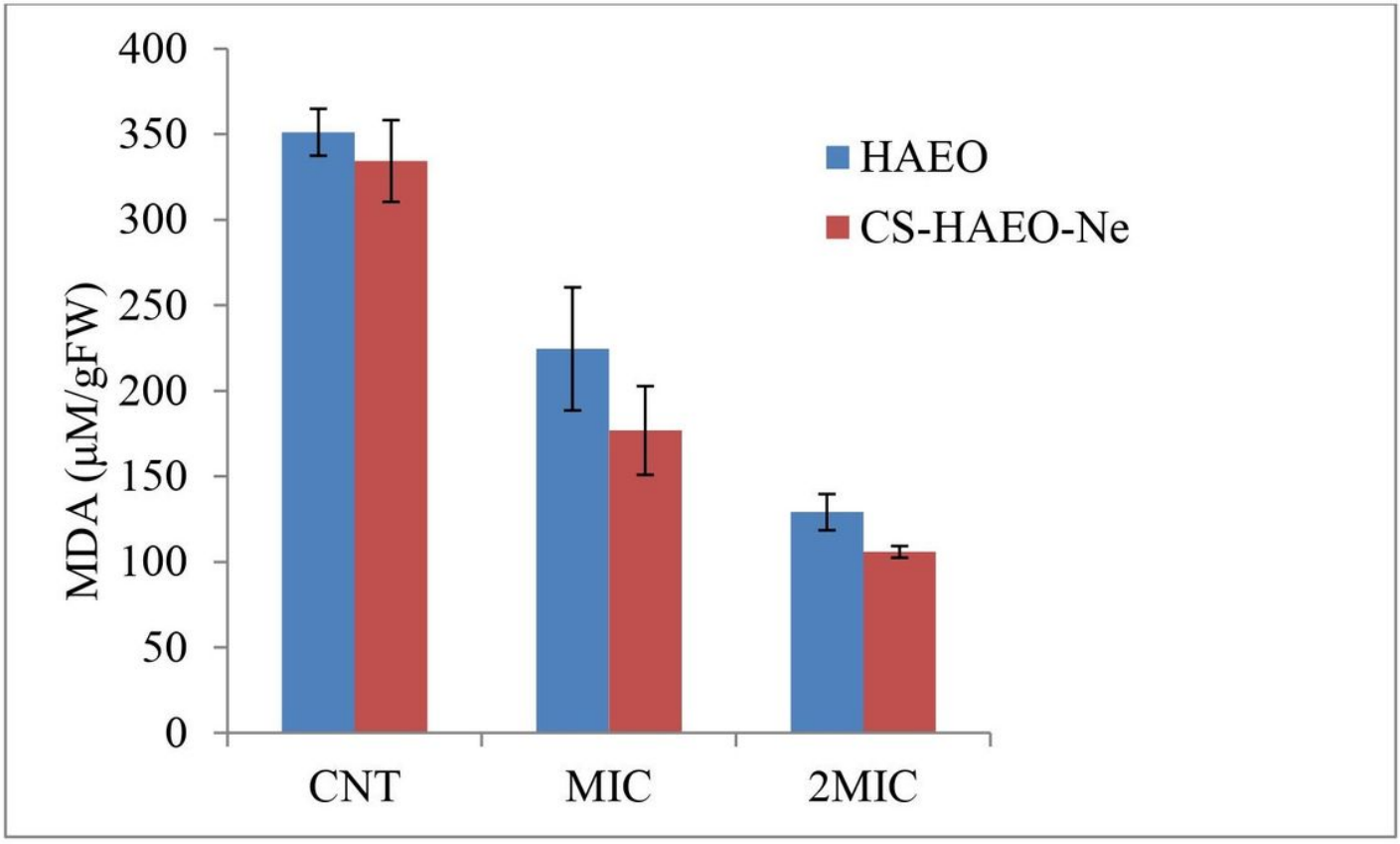

Figure 10

Effect of HAEO and CS-HAEO-Ne fumigation on lipid peroxidation of stored black cumin (Nigella sativa) seeds

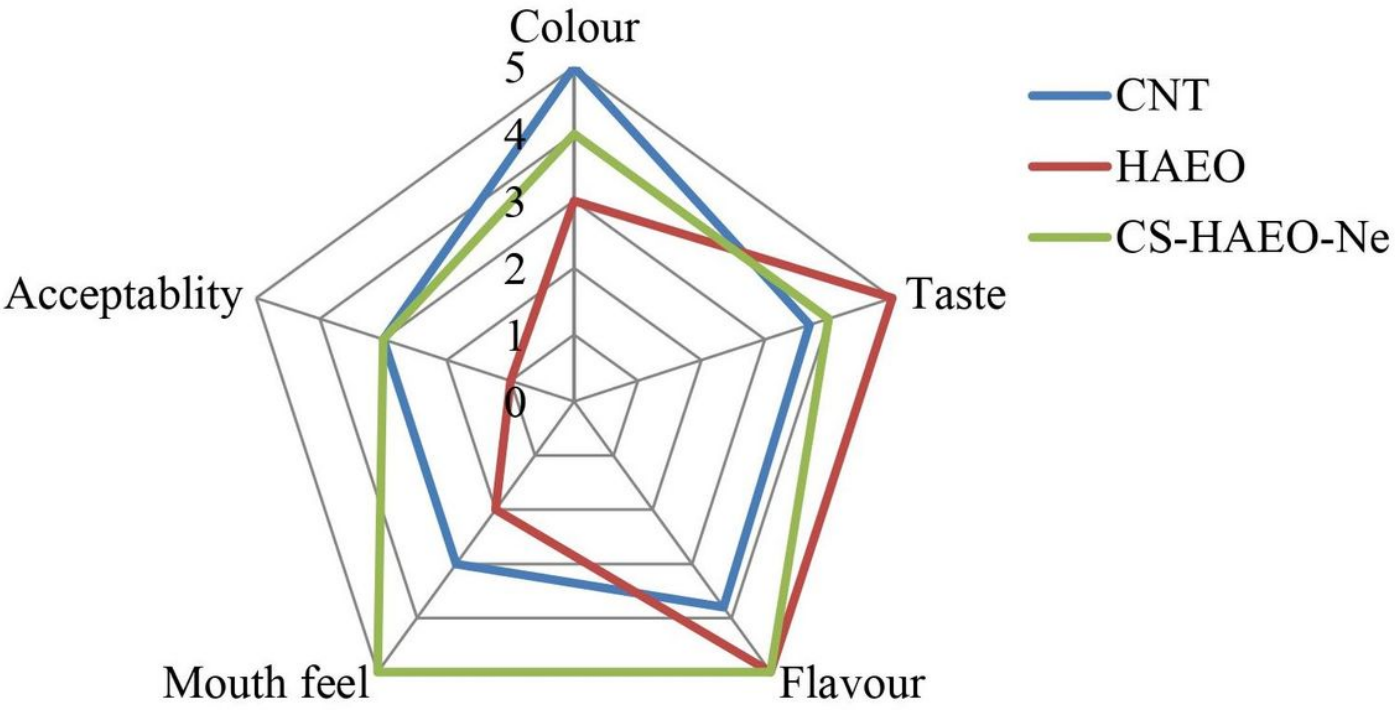

Figure 11

Sensorial profile of HAEO and CS-HAEO-Ne fumigated black cumin (Nigella sativa) seed